Formation and evolution of late-type dwarf galaxies. I. NGC 1705 and NGC 1569

Donatella Romano,[1*] Monica Tosi,[1] and Francesca Matteucci[2]

[1] *INAF – Osservatorio Astronomico di Bologna, Via Ranzani 1, I-40127 Bologna, Italy*
[2] *Dipartimento di Astronomia, Università di Trieste, Via G.B. Tiepolo 11, I-34131 Trieste, Italy*

ABSTRACT
We present one-zone chemical evolution models for two dwarf starburst galaxies, NGC 1705 and NGC 1569. Though especially designed for the inner ~ 1 kpc region, where numerous H II regions and most of the stars are observed, the models also account for the presence of extended gaseous and dark matter haloes, and properly compute the binding energy of the gas heated by supernova explosions. Using information about the past star formation history and initial mass function of the systems previously obtained from *Hubble Space Telescope* optical and near-infrared colour-magnitude diagrams, we identify possible scenarios of chemical enrichment and development of galactic winds. We assume that the galactic winds are proportional to the Type II and Type Ia supernova rates. As a consequence, they do not necessarily go to zero when the star formation stops. In order not to overestimate the current metallicity of the interstellar gas inferred from H II region spectroscopy, we suggest that the winds efficiently remove from the galaxies the metal-rich ejecta of dying stars. Conversely, requiring the final mass of neutral gas to match the value inferred from 21-cm observations implies a relatively low efficiency of interstellar medium entrainment in the outflow, thus confirming previous findings that *the winds driving the evolution of typical starbursts are differential.* These conclusions could be different only if the galaxies accrete huge fractions of unprocessed gas at late times. By assuming standard stellar yields we obtain a good fit to the observed nitrogen to oxygen ratio of NGC 1569, while the mean N/O ratio in NGC 1705 is overestimated by the models. Reducing the extent of hot bottom burning in low-metallicity intermediate-mass stars does not suffice to solve the problem. Localized self-pollution from stars more massive than $60 \, M_\odot$ in NGC 1705 and/or funneling of larger fractions of nitrogen through its winds are then left to explain the discrepancy between model predictions and observations. Inspection of the log(N/O) vs. log(O/H)+12 diagram for a large sample of dwarf irregular and blue compact dwarf galaxies in the literature favours the latter hypothesis. Yet, the physical mechanisms responsible for such a selective loss of metals remain unclear.

Key words: galaxies: abundances – galaxies: evolution – galaxies: formation – galaxies: individual: NGC 1705, NGC 1569 – galaxies: irregular – galaxies: starburst.

1 INTRODUCTION

Low-luminosity galaxies are the most common type of galaxies in the nearby universe (Hodge 1971). Dwarf galaxies present a well pronounced dichotomy between the two main classes of early-type and late-type dwarfs (dwarf irregulars, DIGs, and blue compact dwarfs, BCDs). Indeed, most dwarfs are either gas-poor spheroids with dominant intermediate-age or old stellar populations, or gasrich, star-forming systems (van den Bergh 1977). Only few transition objects are known (Sandage & Hoffman 1991). Here we concentrate on DIGs and BCDs. BCDs are currently undergoing

vigorous star formation (SF) activity. They are objects of compact appearance, with centrally concentrated starburst, gas and star distributions. Part of the extended neutral gas may be kinematically decoupled from the galaxies (van Zee, Skillman & Salzer 1998). DIGs are instead dominated by scattered bright H II regions in the optical, while in H I they show a complicated fractal-like pattern of shells, filaments and clumps. Typical H I masses are $\leq 10^9 \, M_\odot$.

Studying gas-rich starbursting objects helps to better understand the process of star formation from low-metallicity gas clouds and the derivation of the primordial helium abundance with the need for a minimum extrapolation to early conditions (e.g., Peimbert & Torres-Peimbert 1974; Izotov & Thuan 1998). Moreover, by studying dwarf galaxies, one can complement the information available for solar composition stars and get useful insights into the

* E-mail: donatella.romano@bo.astro.it (DR); monica.tosi@bo.astro.it (MT); matteucci@ts.astro.it (FM)

metal dependence of the stellar yields and the winds in Wolf-Rayet (W-R) stars.

Late-type dwarfs have low metallicities, large gas content and mostly young stellar populations: all these features indicate they are poorly evolved objects and are consistent with two possible explanations for their nature: (i) either they are newly formed galaxies or (ii) they have evolved slowly over the Hubble time. In their pioneering work, Searle, Sargent & Bagnuolo (1973) discarded the youth hypothesis and concluded that extremely blue galaxies must have undergone brief but intense bursts of SF separated by long quiescent periods (bursting SF). Recent detections of old underlying stellar populations in most BCDs seem to corroborate Searle's et al. (1973) earlier suggestion and reveal at least another burst of SF besides the present one, even in the case of the most metal-poor BCD known, I Zw 18 (Aloisi, Tosi & Greggio 1999; Östlin 2000; Izotov & Thuan 2004).

Besides the bursting SF mode, gasping (Tosi et al. 1991) or mild continuous (Carigi, Colín & Peimbert 1999; Legrand et al. 2000) SF regimes have been proposed for DIGs and BCDs. The gasping regime, in which the interburst periods last significantly less than the active phases, probably is the more realistic picture for many of them (Schulte-Ladbeck et al. 2001).

Larson & Tinsley (1978) postulated the existence of a close connection between violent dynamical phenomena and bursts of SF. Observational evidence of intense ongoing SF in isolated BCDs (Campos-Aguilar & Moles 1991) contradicts this hypothesis. However, at least some 'isolated' BCDs might have low surface brightness or pure H I companions (Méndez & Esteban 2000; Noeske et al. 2001; Pustilnik et al. 2001; Hoffman et al. 2003). In addition to tidal interactions, low-mass stellar or gaseous companions might trigger and fuel starbursts by infalling on to the DIG (Köppen & Edmunds 1999; cfr. also the 'minor merger' phenomenon described by Sancisi 1999). Another explanation for the intermittent mode of SF in DIGs and BCDs was given by Gerola, Seiden & Schulman (1980), who applied the stochastic self-propagating SF (SSPSF) model to systems of small size. Yet, the high dispersion of the properties of these galaxies cannot be explained in terms of the SSPSF mechanism alone (Matteucci & Chiosi 1983). In particular, galactic winds (GWs) of variable intensity (Matteucci & Chiosi 1983; Matteucci & Tosi 1985) releasing metals in different proportions (enriched winds – Pilyugin 1993; Marconi, Matteucci & Tosi 1994; Carigi et al. 1995) were introduced in order to reproduce the high $\Delta Y/\Delta O$ ratio and the distribution of N/O vs. O/H observed in extragalactic H II regions.

Observational evidence for starburst-driven large-scale outflows was established for a number of starburst or young post-starburst systems, including I Zw 18 (Martin 1996), NGC 1569 (Waller 1991; Heckman et al. 1995), and NGC 1705 (Meurer et al. 1992; Marlowe et al. 1995). This evidence is now growing fast, since diffuse and filamentary gas associated with large-scale outflows are detected for an increasing number of starbursting dwarfs (Veilleux et al. 2003; Cannon et al. 2004). However, whether the final fate of this gas is to eventually escape from the galaxy or to cool and recollapse forming the next generations of stars is not yet clear. *Far Ultraviolet Spectroscopic Explorer (FUSE)* observations of the O VI λ 1032 absorption line arising in the galactic outflow of NGC 1705 suggest that the superbubble has begun to blow out of the interstellar medium (ISM) in the disk of NGC 1705 (Heckman et al. 2001). This superbubble is likely to become a superwind and vent its metals and kinetic energy. The bulk of the global ISM (H I) in NGC 1705 will be retained (Mac Low & Ferrara 1999). A similar scenario should be suitable also for I Zw 18 (Martin 1996). Re-

cently, we have also been provided with the first direct evidence for metal-enriched winds from dwarf starburst galaxies: deep *Chandra* imaging of NGC 1569 has led to an estimated mass of oxygen in the hot wind similar to the oxygen yield of the current starburst (Martin, Kobulnicky & Heckman 2002). The most likely interpretation is that the wind carries nearly all the metals expelled by supernovae (SNe). A similar scenario emerges also from chemodynamical simulations (e.g. Recchi et al. 2004, 2005).

In this paper we study the chemical evolution of DIGs and BCDs. In particular, we compare predictions from models with structural parameters applicable to NGC 1705 and NGC 1569 with their observed properties. Our choice is motivated by the fact that the recent star formation history (SFH), initial mass function (IMF) and chemical enrichment of these two galaxies are rather well constrained by the observations. Therefore, we can construct models without making arbitrary assumptions about the SFH and IMF (which are usually free parameters of the chemical evolution models), and assume the values inferred from the observations. As a consequence, we are able to better constrain other poorly known physical processes which drive galaxy evolution, such as, for instance, the stellar feedback. Both NGC 1705 and NGC 1569 have strong galactic winds, likely triggered by the recent starbursts, and we aim at better understanding how these outflows develop.

The layout of the paper is the following. Observations are presented in § 2, the models are described in § 3, model results are given in § 4 and discussed in § 5. Finally, the conclusions are drawn in § 6.

2   OBSERVATIONS

2.1   General properties of dwarf irregular and blue compact dwarf galaxies

2.1.1   Chemical abundances

Metallicities in DIGs and BCDs are usually derived from the ionized gas in H II regions. From the optical, O, N, S, Ne, Ar, He, and even fainter lines such as those of Fe are measured, while C and Si abundances are obtained from the ultraviolet (UV). Oxygen is the element with the most reliable determinations, since all its most important ionization stages can be observed. The intrinsic uncertainty is of the order of ~ 0.1 dex, which rises at 0.2 dex or more when the electron temperature cannot be directly determined (Pagel 1997). H II regions are ionized by newly born massive stars, hence showing the metallicity of the ISM at the present time. A possible problem with metal-poor H II regions could be self-pollution of fresh metals by winds from young massive stars, so that the abundances inferred from the nebular emission lines would not be representative of that in the local ISM (Kunth & Sargent 1986; Pagel, Terlevich & Melnick 1986). However, if the elements ejected from massive stars are in high ionization stages, they are not expected to significantly contribute to the element abundances as derived from optical lines (Pantelaki & Clayton 1987). Observational evidence for this comes from the chemical homogeneity of most star-forming galaxies, in which the expected spatial variations in oxygen abundances are not observed, despite the presence of multiple massive star clusters (Kobulnicky & Skillman 1997, 1998).

Recently, a step forward in understanding the physical and chemical evolution of dwarf star-forming galaxies has been accomplished thanks to *FUSE*, which makes possible the determination of the metal abundances of the neutral ISM of these galaxies. Preliminary data analysis points to an offset in metal content between the

neutral ISM and H II regions, at least for the galaxies surveyed up to now (Aloisi et al. 2005). We naturally find a qualitative explanation for this offset in the framework of our model (see discussion in Sect. 4). However, many uncertainties still affect both the interpretation of the data and the physics of the model, thus making the accurate quantification of the offset a hardly achievable goal.

Only for the closest galaxies, there is the possibility of tracing the history of the chemical enrichment of the ISM through spectroscopy of the resolved stellar populations (Hill 2004; Tolstoy et al. 2004, and references therein). Photometric estimates of the iron stellar abundances can be obtained from colour-magnitude diagrams (CMDs), but with much lower reliability.

2.1.2 Star formation history and initial mass function

The synthetic CMD method (Tosi et al. 1991; see also Gallart et al. 1994; Tolstoy & Saha 1996; Aparicio & Gallart 2004 and references therein) allows one to estimate the epochs and intensities of the SF activity in a galaxy, as well as the IMF slope.

In galaxies outside the Local Group, crowding and magnitude limits make it increasingly difficult to resolve the fainter stars and shorten accordingly the reachable look-back time. Nevertheless, their SFHs have been inferred up to a few Gyr ago (Tosi 2003, and references therein).

The following sections, Sects. 2.2.1 and 2.2.2, are mostly devoted to a detailed description of the SFHs, IMF slopes, and chemical abundances inferred for NGC 1705 and NGC 1569. In spite of being differently classified (as a BCD NGC 1705 and as a DIG NGC 1569), they are otherwise similar objects, showing both evidence of a complex structure and the presence of galactic outflows.

2.2 Individual objects

2.2.1 NGC 1705

NGC 1705 is a nearby, isolated BCD. Its nuclear region contains an extremely luminous super star cluster (SSC), responsible for about half of the total UV light from the galaxy (Meurer et al. 1992). SF is found to occur now, mainly concentrated in the high surface brightness part of the galaxy (Annibali et al. 2003). In this region, the presence of W-R emission lines suggests ongoing SF during the past 5 Myr (Meurer et al. 1992). In Hα, NGC 1705 shows a bipolar morphology, suggesting an outflow powered by the recent SF activity in the nucleus (Meurer et al. 1992). UV absorption-line kinematics bears witness to this too (Heckman & Leitherer 1997). The gas metallicity, as derived from UV, optical and near infrared (NIR) spectra of H II regions is 12+log(O/H) = 8.36 (Storchi-Bergmann, Calzetti & Kinney 1994), corresponding to $Z \simeq 0.004$ (for $Z_\odot = 0.017$), close to the metallicity of the SMC. A higher value, 12+log(O/H) $\sim$ 8.46, is reported by Meurer et al. (1992), while Heckman et al. (1998) give 12+log(O/H) $\simeq$ 8.0. Recently, Lee & Skillman (2004) have derived a mean oxygen abundance of 12+log(O/H) = 8.21 $\pm$ 0.05. They have detected [O III] λ 4363 in five H II regions of NGC 1705, which makes their oxygen determination highly reliable, thanks to the direct measurements of electron temperatures. The estimated log(N/O) = -1.75 ± 0.06 is among the lowest values ever observed for dwarf irregulars, but it raises up to -1.63 ± 0.07 if the anomalously low nitrogen abun-

Table 1. NGC 1705 identity card.

Quantity	Observed value		References
D	5.1 ± 0.6 Mpc		1
$R_{\rm H}$	1.7 kpc[a]		2
$M_{\rm gas}$	1.7×10^8 M$_\odot$ [a]		3
$M_{\rm stars}$	1.7×10^8 M$_\odot$ [a]		3
Z	0.004		4
	H II regions	Neutral ISM	
log(O/H) + 12	8.46		3
	8.36		4
	8.0		5
	8.21 ± 0.05	7.50 ± 0.01[b]	6, 7
log(N/H) + 12	6.46 ± 0.08	5.68 ± 0.06	6, 7
log(Fe/H) + 12		6.21 ± 0.03	7
log(N/O)	-1.75 ± 0.06[c]	-1.82 ± 0.07	6, 7
	-1.62		4
log(Ne/O)	-0.426 ± 0.033		6

1– Tosi et al. 2001; 2– Meurer et al. 1998; 3– Meurer et al. 1992; 4– Storchi-Bergmann et al. 1994; 5– Heckman et al. 1998; 6– Lee & Skillman 2004; 7– Aloisi et al. 2005.

[a] Radius and masses were modified to reflect the distance used here.

[b] The oxygen abundance is that derived from the total (neutral plus ionized) absorbing gas. That referring to the sole neutral gas would be somehow lower.

[c] log(N/O) = -1.63 ± 0.07 if the anomalously low nitrogen value in region B4 is ignored (see Lee & Skillman 2004).

Table 2. Average SFRs at various epochs for NGC 1705 as inferred from the observations (Annibali et al. 2003).

SFR (M$_\odot$ yr^{-1})	Look-back time (Myr)
5.6×10^{-2}	1000–5000
5.8×10^{-2}	50–1000
7.7×10^{-3}	15–50
6.8×10^{-2}	10–15
0.314	0–3

dance in H II region B4 is ignored[†]. In any case, we caution that nitrogen could not be determined in the same regions where direct electron temperatures were available. *FUSE* spectra seem to suggest that the N/O ratio in H I is pretty much the same, while the oxygen content is lower in the cold gas (Aloisi et al. 2005).

Deep and accurate photometry has allowed to resolve stars from the most central regions to the extreme outskirts (Tosi et al. 2001), so that it has been possible to divide the galaxy in several roughly concentric regions and to derive the SFH for each of them (Annibali et al. 2003): (i) different zones of the galaxy experienced different SFHs; (ii) the derived SF is almost continuous with fluctuations in the SFR (i.e., gasping rather than bursting); (iii) the young population dominates in the inner regions, where a recent, intense burst occurred; (iv) the strength of the most recent activity gradually decreases moving from the central to the outer regions; (v) NGC 1705 is definitely not a young galaxy: an old population is spread over the whole galaxy (see also Meurer et al. 1992); (vi) the

[†] Notice that a value of log(N/O) = -1.63 ± 0.07 is in excellent agreement with the previous estimate by Storchi-Bergmann et al. (1994) – see Table 1, second-last row.

total stellar mass astrated in the galaxy is $\sim 3 \times 10^8$ M$_\odot$ and ~ 20 per cent of the stars are younger than 1 Gyr; (vii) a Salpeter ($x = 1.35$) or slightly steeper ($x = 1.6$) field star IMF provides the best agreement with the observations.

In Table 1 we summarize some structural parameters and observed properties of NGC 1705. Listed are: the distance to NGC 1705, D; its Holmberg radius, $R_{\rm H}$; its total atomic gas mass (H I + He), $M_{\rm gas}$; its stellar mass, $M_{\rm stars}$; its present-day metallicity, Z, and the mean oxygen, nitrogen, iron and neon abundances measured in H II regions and neutral gas. Table 2 reports the average SFRs in representative age bins for the whole surveyed area, ~ 12.5 kpc^2, as listed in Annibali et al. (2003 – their table 6, last row).

2.2.2 NGC 1569

NGC 1569 is an exceptionally active DIG, which contains three SSCs (De Marchi et al. 1997; Origlia et al. 2001; Sirianni et al. 2005) and many H II regions out of the SSC zone, where the SF is active now (Waller 1991). According to Aloisi et al. (2001), young stars ($m > 8$ M$_\odot$, $\tau_m < 50$ Myr) are mostly clustered around the three SSCs, whereas intermediate-age objects ($1.9 < m/$M$_\odot < 8$, 50 Myr $< \tau_m < 1$ Gyr) are more evenly distributed. Older stars ($m < 1.9$ M$_\odot$, $\tau_m > 1$ Gyr) are visible at the outskirts of the starbursting region. Filaments are found at different wavelengths and a strong spatial correlation is present between the extended X-ray emission and the Hα filaments detected in the optical (Martin et al. 2002). In H I, a dense, clumpy ridge distribution appears, surrounded by more extended, diffuse neutral hydrogen. Discrete features such as arms and bridges are observed (Stil & Israel 2002) and the dust properties (Galliano et al. 2003) are consistent with the presence of shocks. Perhaps, the galaxy is presently ingesting a companion gaseous cloud (Stil & Israel 1998; Mühle et al. 2005), and it is tempting to speculate upon the enhanced SF to coincide with the accretion episode. Recent SN explosions triggered a GW (Martin et al. 2002), but it is unlikely that it will efficiently remove the ISM, unless stripping or other environmental factors intervene (D'Ercole & Brighenti 1999; see also Mac Low & Ferrara 1999). *Chandra* observations reveal large inhomogeneities in the metal abundance of the ISM, with Z ranging from 0.1 to 1 $Z_\odot$ (Martin et al. 2002), again suggesting that multiple SN explosions from recent starbursts polluted the ISM.

The SFH of NGC 1569 has been extensively studied in the last decade. Vallenari & Bomans (1996), from V and I optical bands, find that a global SF episode occurred from 100 to 4 Myr ago. They find hints for an older episode (from 1.5 Gyr to 150 Myr ago) and rule out the existence of long-lasting quiescent phases in the last 1.5 Gyr. Similarly, based on B and V bands, Greggio et al. (1998) derive for the most recent burst – which, in the examined region, ended from 5 to 10 Myr ago – a duration of ≥ 100 Myr and a very high rate, ~ 0.5 M$_\odot$ yr^{-1} in the inner ~ 0.14 kpc^2 of the galaxy if Salpeter's IMF is assumed over the 0.1–120 M$_\odot$ stellar mass range. If quiescent periods occurred, they lasted less than ~ 10 Myr. By using NIR data, Angeretti et al. (2005) looked deeper backward in time and found three major episodes of SF in the last 1 (possibly 2) Gyr. They are able to distinguish two episodes at least for the most recent SF activity. The first started ~ 150 Myr ago and ended ~ 40 Myr ago. The second formed stars between 37 and 13 Myr ago, at a mean rate about 3 times higher than the preceding one, i.e. ~ 0.13 M$_\odot$ yr^{-1} if Salpeter's IMF is assumed, in agreement with previous literature data. From their *Hubble Space Telescope (HST)* NICMOS/NIC2 data, the same authors also find evidence for a gap

Table 3. NGC 1569 identity card.

Quantity	Observed value	References
D	2.2 ± 0.6 Mpc[a]	1
d	1.85 kpc	2
$M_{\rm gas}$	$(1.5 \pm 0.3) \times 10^8$ M$_\odot$	1
$M_{\rm tot}$	3.3×10^8 M$_\odot$	1
μ	0.46 ± 0.09	1
	0.264–0.73	3, 4
Z	0.004	5
(He/H)	0.080 ± 0.003[b]	6
$\log({\rm O/H}) + 12$	8.19–8.37	6, 7, 8
$\log({\rm N/O})$	-1.39 ± 0.05	6
	-0.81	8
SFR	~ 0.5 M$_\odot$ yr^{-1}[c]	9
	0.32 M$_\odot$ yr^{-1}	10

1– Israel 1988; 2– Stil & Israel 2002; 3– Lee et al. 2003a; 4– Martin et al. 2002; 5– González Delgado et al. 1997; 6– Kobulnicky & Skillman 1997; 7– Martin 1997; 8– Storchi-Bergmann et al. 1994; 9– Greggio et al. 1998; 10– Hunter & Elmegreen 2004.

[a] Recently, Makarova & Karachentsev (2003) have derived from the I magnitude of the tip of the RGB two possible values for the distance to NGC 1569, 1.95 ± 0.2 Mpc and 2.8 ± 0.2 Mpc.

[b] The error bar is likely to be larger (see Olive & Skillman 2004 reanalysis of helium abundance determinations in extragalactic H II regions).

[c] The tabulated value refers to a look-back time of 0.1–0.15 Gyr. It has been derived for the central ~ 0.14 kpc^2 of the galaxy, assuming a Salpeter IMF. The data also indicate a halt in the SFR 5–10 Myr ago. Strong SF activity is expected between 1.5 and 0.15 Gyr ago.

in the SF activity (or, alternatively, for a low-level SF) from 300 to 150 Myr ago, and traces of an older SF episode, occurred about 1–2 Gyr ago at a rate between 0.01 and 0.06 M$_\odot$ yr^{-1} (depending on the assumed duration). The relatively recent, strong SF activity proceeded at rates that could have not been sustained over a Hubble time, since it would have consumed all the available gas in ~ 1 Gyr, or even less (Greggio et al. 1998). Although a low-level SF is not excluded in the past, certainly the last 1–2 Gyr have been peculiar in the SFH of NGC 1569. There is an overall agreement among the various SFHs inferred from different bands.

In a recent work, Anders et al. (2004) from multi-colour archive *HST* data show that a high level of star cluster formation started ~ 25 Myr ago in NGC 1569, while a lower level of activity characterized older epochs, with a secondary peak ~ 100 Myr ago. The age distribution of star clusters displays a gap in the age interval 160–400 Myr. Heckman et al. (1995) find that observations of the expanding superbubbles in NGC 1569 can be fairly well explained assuming a SF episode at a constant rate over the ages 13–32 Myr, which are very similar to those inferred by Angeretti et al. (2005) for their youngest burst. Hunter & Elmegreen (2004) find a present-day SFR $\psi(t_{\rm now}) \simeq 0.32$ M$_\odot$ yr^{-1} from Hα imaging.

For reference, in Table 3 we summarize some basic observational properties of NGC 1569. Listed are: the distance to NGC 1569, D; its maximum optical size, d; its total atomic gas mass (H I + He), $M_{\rm gas}$; its total mass, $M_{\rm tot}$; the ratio between the latter two, μ, which shows that from 1/4 to 3/4 of the total mass eventually resides in neutral atomic gas, depending on different authors; the total metal, helium, oxygen and nitrogen abundances in the ISM of NGC 1569 and, finally, a lower limit to the intensity of the latest SF episode, according to optical data. It is worth noticing that the N/O ratio measured by Kobulnicky & Skillman (1997)

for NGC 1569 is significantly lower than that derived by Storchi-Bergmann et al. (1994). We will compare only the more recent, more accurate determinations to our model predictions.

3 MODELS

In order to study the formation and evolution of late-type dwarfs, we use an updated version of the galactic chemical evolution (GCE) model developed by Bradamante, Matteucci & D'Ercole (1998). In particular: (i) we adopt up-to-date stellar yields, (ii) we revise the prescriptions about the GWs, and (iii) we treat the infall of primordial gas as a free parameter. The adopted SFH and IMF are those inferred from previous CMD analyses, less prone to *ad hoc* assumptions.

The main features of the model are the following:

(i) the model is one zone with instantaneous and complete mixing of gas inside it;

(ii) the instantaneous recycling approximation is relaxed, i.e. the stellar lifetimes are taken into account in detail;

(iii) GWs originate when the thermal energy of the gas equates its binding energy;

(iv) the winds preferably expel metals from the galaxy, while retaining large fractions of hydrogen;

(v) the GW efficiency varies with time according to the SN (II plus Ia) rate predicted by the model.

3.1 General prescriptions

Homogeneity and instantaneous mixing of gas are reasonable working hypotheses, as long as gradients are not observed in the galaxy and the cooling time of the gas proves to be short enough. Hydrodynamical simulations of the behaviour of the ISM and the metals ejected by massive stars after a starburst suggest that most of the metals effectively cool off in a few million years (Hensler et al. 2004; Recchi et al. 2001)‡. The existence of a small age gap between previous SF activity and the latest ongoing burst in NGC 1705 ($\sim$ 6 million years; see Table 2) is consistent with quite short time scales for gas cooling as well. Yet, the low occurrence of localized chemical pollution in the vicinity of young star clusters in star-forming dwarfs (see Sect. 2.1.1) points to time scales for metals cooling longer than $\sim 10^7$ yr (Kobulnicky & Skillman 1997).

Galactic outflows develop when the thermal energy of the gas, $E_{\rm th}$, equates its binding energy, $E_{\rm b}$. Following Bradamante et al. (1998), the thermal energy of the gas grows as a consequence of SF activity due to energy injection from stellar winds and SN explosions (both Type II and Type Ia SNe are considered):

$$E_{\rm th}(t) = \eta_{\rm SNII} E_{\rm SN} \int_0^t R_{\rm SNII}(t')\,{\rm d}t' \ +$$
$$+ \ \eta_{\rm SNIa} E_{\rm SN} \int_0^t R_{\rm SNIa}(t')\,{\rm d}t' \ +$$
$$+ \ \eta_{\rm wind} E_{\rm wind} \int_0^t \int_{12}^{100} \varphi(m)\psi(t')\,{\rm d}m\,{\rm d}t'. \qquad (1)$$

---

‡ Notice that these results strongly rest on the assumed (low) heating efficiency of SNeII, i.e. on the (low) fraction of the SN explosion energy which remains effectively stored in the ISM and is not radiated away, $\eta_{\rm SNII} = 0.03$. The larger $\eta_{\rm SNII}$, the longer the cooling time of the ejecta.

$\varphi(m)$ is the IMF, $\psi(t)$ is the SFR, $E_{\rm SN} = 10^{51}$ erg is the total energy released by a typical SN explosion, $E_{\rm wind} = 10^{49}$ erg is the total energy injected into the ISM by a typical massive star through stellar winds. $R_{\rm SNII}(t)$ and $R_{\rm SNIa}(t)$ are the rates of SN explosions, which are computed according to Matteucci & Greggio (1986). $\eta_{\rm SNII}$, $\eta_{\rm SNIa}$ and $\eta_{\rm wind}$ represent the efficiencies with which the energies of the stellar explosions and stellar winds are transferred into the ISM. According to Recchi et al.'s (2001, 2004) chemodynamical results for I Zw 18, the efficiencies of energy transfer for Type II SNe, Type Ia SNe and stellar winds are $\eta_{\rm SNII} = 0.03$, $\eta_{\rm SNIa} = 1.0$ and $\eta_{\rm wind} = 0.03$, respectively (since SNeIa explode in a hotter medium, rarefied by previous SNII explosions, their energy is more efficiently thermalized). However, in case of protracted SF, it is likely that SNe of both types meet with the same ISM conditions. Therefore, $\eta_{\rm SNII} \simeq \eta_{\rm SNIa}$ would be a more reasonable choice. We test both hypotheses in our study. The binding energy of the gas is a function of the assumed dark matter (DM) content and distribution. A massive ($M_{\rm d}/M_{\rm lum} = 10$) diffuse ($R_{\rm eff}/R_{\rm d} = 0.1$) dark halo is assumed, where $M_{\rm d}$ and $M_{\rm lum}$ are the dark and luminous mass, respectively, and $R_{\rm eff}$ and $R_{\rm d}$ are the effective radius and the radius of the DM core (see Table 4). Once the conditions for the onset of a galactic-scale outflow are met, metals are assumed to be lost more easily than the neutral hydrogen. This is expected on the basis of the geometry and mass of the system: flattened galaxies of 10^8–10^9 M$_{\odot}$ loose preferentially metal-enriched matter along the polar direction, while the unprocessed gas remains almost unperturbed (De Young & Gallagher 1990; Mac Low & Ferrara 1999; D'Ercole & Brighenti 1999; Recchi et al. 2001; Marcolini, Brighenti & D'Ercole 2004). Most of the metal-rich ejecta are pushed to large distances from the galaxy (of the order of several kpc), but their final fate is uncertain: they could either cool and fall back on to the galaxy plane, or be removed from the galaxy. Hydrodynamical simulations of the interaction between SN-powered gas outflows and the local intergalactic medium (IGM) in fiducial galaxies resembling dwarf spheroidals show that ram pressure and tidal stripping can efficiently pull away matter loosely bound to the galaxy (Murakami & Babul 1999). If a flattened rather than a spherical ISM distribution is assumed, the fraction of metals retained by a moving galaxy is found to be up to three times larger than that retained by a galaxy at rest (Marcolini et al. 2004). This is interesting in the light of the empirical evidence that dwarf spheroidals are depleted of their gas, whereas DIGs and BCDs still show large gaseous contents.

We follow in detail the time evolution of several chemical species (H, D, He, C, N, O, Mg, Si, S, Ca and Fe), by means of the following basic equation:

$$\frac{{\rm d}\mathcal{G}_i(t)}{{\rm d}t} = -X_i(t)\psi(t) + \mathcal{R}_i(t) + \frac{{\rm d}\mathcal{G}_i^{\rm inf}(t)}{{\rm d}t} - \frac{{\rm d}\mathcal{G}_i^{\rm out}(t)}{{\rm d}t}, \qquad (2)$$

where $\mathcal{G}_i(t) = X_i(t)M_{\rm gas}(t)/M_{\rm nor}$ is the fractional gas mass in the form of the element i at the time t, normalized to a fixed total mass, $M_{\rm nor}$. The quantity $X_i(t)$ represents the abundance by mass of the element i at the time t and the summation over all the elements in the gas mixture is equal to unity. $\psi(t)$ is the SFR, while $\mathcal{R}_i(t)$ represents the fraction of mass which is restored into the ISM in the form of the element i by dying stars. A detailed description of this term, which contains all the prescriptions about the stellar IMF, stellar nucleosynthesis and Type Ia SN progenitors, can be found in Matteucci & Greggio (1986). The specific yield sets adopted in this work are discussed in Sect. 3.2. Finally, the last two terms on the right-hand side of Equation (2) account for possible gas inflows and outflows, respectively.

Table 4. Parameters of the models with their adopted values.

Parameter	Meaning	Adopted value	
		NGC 1705	NGC 1569
$M_{\rm nor}$	normalizing mass (gaseous matter available for accretion inside the DM potential)	7×10^8 M$_\odot$	5×10^8 M$_\odot$
$M_{\rm d}$	DM amount	7×10^9 M$_\odot$	5×10^9 M$_\odot$
$R_{\rm eff}$	effective radius of the visible matter	1.2 kpc	1 kpc
$R_{\rm eff}/R_{\rm d}$	effective to DM core radii ratio	0.1	
τ	time scale for mass accretion	8 Gyr	0.5, 5 Gyr
$\eta_{\rm SNII}$	SNII thermalization efficiency	0.20	0.03, 0.20, 0.50
$\eta_{\rm SNIa}$	SNIa thermalization efficiency	0.20	0.20, 0.50, 1.00
$\eta_{\rm wind}$	stellar wind thermalization efficiency	0.20	
$t_{\rm now}$	age of the universe	13.7 Gyr	

In many literature models for dwarf galaxy formation, DIGs and BCDs form from continuous infall of gas of primordial chemical composition, until a mass from a few 10^8 M$_\odot$ up to $\sim 10^9$ M$_\odot$ is accumulated. The rate of gas infall is normally parametrized as

$$\frac{\mathrm{d}\mathcal{G}_i^{\rm inf}(t)}{\mathrm{d}t} = \frac{X_i^{\rm inf} e^{-t/\tau}}{\tau(1 - e^{-t_{\rm now}/\tau})}, \tag{3}$$

with τ, the infall time scale, being the most critical free parameter and largely varying amongst different authors (e.g., $\tau = 0.5$ Gyr for Matteucci & Tosi's 1985 models; $\tau = 1, 4, 7$ Gyr for Mouhcine & Contini's 2002 models). Here we run models with the choices for τ specified in Table 4. $X_i^{\rm inf} = X_i^{\rm P}$ is the primordial abundance of element i in the inflowing gas. Here we adopt (D/H)$_{\rm P} = 2.5 \times 10^{-5}$, (^{3}He/H)$_{\rm P} = 0.9 \times 10^{-5}$, and $Y_{\rm P} = 0.248$ (see Romano et al. 2003, and references therein). The quantity $t_{\rm now}$, the present time, is set to 13.7 Gyr. In addition, we test also the cases of a constant infall rate,

$$\frac{\mathrm{d}\mathcal{G}_i^{\rm inf}(t)}{\mathrm{d}t} = {\rm const}, \tag{4}$$

and of an increasing exponential,

$$\frac{\mathrm{d}\mathcal{G}_i^{\rm inf}(t)}{\mathrm{d}t} = \frac{X_i^{\rm inf} e^{t/\tau}}{\tau(e^{t_{\rm now}/\tau} - 1)}, \tag{5}$$

with the lowest accretion rates at the early stages of galaxy formation and the highest ones at later epochs, to coincide with the observed late SF boosting. Notice that the infall rate is normalized to the quantity $M_{\rm nor}$, which obeys the condition: $M_{\rm nor} = M_{\rm gas}(t_{\rm now}) + M_{\rm stars}(t_{\rm now}) + M_{\rm rem}(t_{\rm now}) + M_{\rm GW}(t_{\rm now})$, where $M_{\rm gas}(t_{\rm now})$, $M_{\rm stars}(t_{\rm now})$, and $M_{\rm rem}(t_{\rm now})$ are the masses in form of gas, stars and stellar remnants, respectively, and $M_{\rm GW}(t_{\rm now})$ is the total mass ejected from the galaxy by GWs at the present time.

The rate of gas loss via GWs at the time t is assumed to be proportional to the amount of gas present at that time. For each element i,

$$\frac{\mathrm{d}\mathcal{G}_i^{\rm out}(t)}{\mathrm{d}t} = w_i(t) X_i^{\rm out}(t) \mathcal{G}(t), \tag{6}$$

where $X_i^{\rm out}(t) = X_i(t)$. Here we call for a dependence of $w_i(t)$ on time via a dependence on the Type II plus Type Ia SN rate (expressed in number Gyr^{-1}):

$$w_i(t) = \beta_i[\eta_{\rm SNII} R_{\rm SNII}(t) + \eta_{\rm SNIa} R_{\rm SNIa}(t)]. \tag{7}$$

The parameter β_i is a proportionality constant indicating the efficiency of mass loss for a specific element i. In the case of differential winds, the value of β_i is assumed to be different for different elements. In particular, higher β_i values are assigned to heavy elements produced in SNe, while only a minor fraction of the neutral hydrogen is allowed to leave the galaxy.

The SFR has the simple form:

$$\psi(t) = \nu\mathcal{G}(t), \tag{8}$$

where ν, the efficiency of SF, is expressed in units of Gyr^{-1}, and is fixed so as to recover the SFR inferred from the observations.

The adopted IMF (by mass) is an extension of that originally proposed by Salpeter (1955) to the whole stellar mass range:

$$\varphi(m) = \mathcal{C} m^{-x}, \tag{9}$$

with $x = 1.35$ for $0.1 \leq m/{\rm M}_\odot \leq 100$. $\mathcal{C}$ is the normalization constant, and is obtained by imposing the condition

$$\int_{0.1}^{100} \varphi(m)\mathrm{d}m = 1. \tag{10}$$

This IMF is in agreement with the results of the CMD analysis for both NGC 1705 and NGC 1569, though one must be aware that *the synthetic CMDs actually constrain the IMF slope of these galaxies only for $m \gtrsim 6\,M_\odot$* (Annibali et al. 2003). Flatter slopes in the low-mass range cannot be excluded (Angeretti et al. 2005). We discuss the effect on model results of adopting different IMF formulations – still consistent with the CMD analysis – in Sect. 4.3.1.

3.2 Nucleosynthesis prescriptions

To quantitatively estimate the uncertainty on the results related to different nucleosynthesis assumptions, we have run our models assuming various sets of stellar yields.

For low- and intermediate-mass stars (LIMS), i.e., stars with $0.8 \leq m/{\rm M}_\odot \leq 8$, both the yields of van den Hoek & Groenewegen (1997) and those computed by Meynet & Maeder (2002) for rotating stellar models are considered. For the van den Hoek & Groenewegen (1997) yields, we adopt either those computed with constant mass loss parameter along the asymptotic giant branch (AGB), $\eta_{\rm AGB} = 4$ (Table 5; models labelled N), or those computed with metallicity-dependent $\eta_{\rm AGB}$ (Table 5; models labelled W), or those computed with the minimum hot bottom burning (HBB) extent allowed by the observations (Table 5; models labelled H). For the Meynet & Maeder (2002) yields, we adopt those computed for initial rotational velocities of the stars of $v_{\rm ini} = 300$ km s^{-1} (Table 5; models labelled M).

For massive stars, i.e., stars with $m > 8$ M$_\odot$, the adopted nucleosynthesis prescriptions are either from Nomoto et al. (1997; Table 5; models N and H), or from Woosley & Weaver (1995;

Table 5. SFH, GW efficiency and nucleosynthesis prescriptions.

		Star formation history		
Model	Number of bursts	Time of burst occurrence (Gyr)	Duration of the burst (Gyr)	ν (Gyr^{-1})
1		Star formation history from Annibali et al. (2003)		
2	3	5.55/11.55/13.6	6/2/0.1	0.05/0.15/2
3	3	5.55/12.55/13.6	6/1/0.1	0.05/0.3/3
4	5	4.575/6.575/8.575/11.55/13.6	0.25/0.25/0.25/2/0.1	0.5/0.5/0.5/0.15/2
5	3	0.7/11.55/13.6	10.5/2/0.1	0.012/0.15/2.4

	GW ejection efficiencies (β_i)[a]	
	H, D, He	C, N, O, and heavier
a	2×10^{-6}	2×10^{-5}
b	2×10^{-6}	2.5×10^{-5}
c	As above, except for nitrogen, for which $\beta_N = 5.5 \times 10^{-5}$	
d	0.5×10^{-5}	2.5×10^{-5}
e	0.5×10^{-5}	1.5×10^{-5}
f	As case *d*, except for nitrogen, for which $\beta_N = 5.5 \times 10^{-5}$	

	Nucleosynthesis prescriptions	
	LIMS	Massive stars
N	van den Hoek & Groenewegen 1997, η_{AGB} const	Nomoto et al. 1997[b]
W	van den Hoek & Groenewegen 1997, η_{AGB} var	Woosley & Weaver 1995[b]
H	van den Hoek & Groenewegen 1997, minimum HBB	Nomoto et al. 1997[b]
M	Meynet & Maeder 2002[c]	Meynet & Maeder 2002[c]

[a] Notice that the actual GW ejection efficiencies are given by $w_i(t) = \beta_i[\eta_{SNII}R_{SNII}(t) + \eta_{SNIa}R_{SNIa}(t)]$, where $R_{SNII}(t)$ and $R_{SNIa}(t)$ are the Type II and Type Ia SN rates by number at time t, respectively, each one multiplied by the appropriate SN heating efficiency.

[b] The yields of ^{12}C for stars more massive than 40 M$_\odot$ were multiplied by a factor of 3 in order to fit the Milky Way carbon abundance data (Chiappini et al. 2003a).

[c] We adopt the set of yields computed for initial rotational velocities of the stars of $v_{ini} = 300$ km s^{-1}.

Table 5; models labelled W), or from Meynet & Maeder (2002; Table 5; models labelled M).

Type Ia SN nucleosynthesis is accounted for by adopting the prescriptions by Thielemann, Nomoto & Hashimoto (1993), their model W7.

Each model is characterized by one number and one pair of letters; the number refers to the adopted SFH, the small letter to the adopted GW efficiency (which, according to the differential wind picture, is higher for the heavy elements than for the light ones), the capital letter to the adopted stellar yields (see Table 5).

4 RESULTS

Most GCE studies published so far assume that DIGs and BCDs evolve through successive bursts of SF – which possibly induce GWs – alternating long quiescency periods (Matteucci & Chiosi 1983; Matteucci & Tosi 1985; Pilyugin 1993; Marconi et al. 1994; Bradamante et al. 1998). Very few attempts are made at modelling specific objects (e.g., Carigi et al. 1999; Recchi et al. 2001, 2004, 2005). However, given the high number of free parameters involved in dwarf galaxy modelling, it is instead of fundamental importance to model individual galaxies whose SFH and IMF have been derived from observations.

4.1 NGC 1705

NGC 1705 has its SFH and IMF slope known thanks to deep *HST* photometry probing epochs up to 5 Gyr ago (see Sect. 2.2.1). The stellar mass astrated at the inferred SFR over the last 5 Gyrs is sufficient to account for the stellar mass we observe in the galaxy to-

day (Annibali et al. 2003). Therefore, there is no need to speculate upon earlier SF activity, and we can safely assume that the galaxy formed the vast majority of its stars during the last ~ 5 Gyrs at the average rates suggested by Annibali et al. (2003; see Table 2). Following those authors, the stellar masses are distributed according to a Salpeter IMF ($x = 1.35$) over the whole (0.1–100 M$_\odot$) stellar mass range, unless otherwise stated.

In Fig. 1 we show the adopted SFH together with some results from Model *1aN*. The adopted structural parameters of the model are: $M_{nor} = 7 \times 10^8$ M$_\odot$, $R_{eff} = 1.2$ kpc, $M_d = 7 \times 10^9$ M$_\odot$, $R_{eff}/R_d = 0.1$ (see Sect. 3.1 and Table 4 for explanations regarding model parameters). The assumed infall law is exponentially decreasing with time with e-folding time $\tau = 8$ Gyr (Fig. 1f, *dashed line*). This is a quite long time scale, comparable to that for the formation of the solar neighbourhood ($\tau_{SN} = 7$ Gyr; Chiappini, Matteucci & Gratton 1997). It allows a non-negligible fraction of the cold gas to be available for SF at late times. The assumed thermalization efficiencies from SNe and stellar winds are $\eta_{SNII} = \eta_{SNIa} = \eta_{wind} = 0.20$.

Model *1aN* well reproduces the present-day gaseous (Fig. 1a) and stellar (Fig. 1c) contents of NGC 1705, as well as its current metallicity (Fig. 1d). In the framework of this model, a galactic outflow develops very soon, already ~ 250 million years after the onset of the SF, due to the strong SN feedback. We predict a current mass loss rate of ~ 0.04 M$_\odot$ yr^{-1} through the outflow, i.e., about an order of magnitude lower than the present-day SFR. This is due to the fact that SNe with progenitors born during the last sudden burst of SF, have not had time to explode and leave their signature on the GW properties yet. Therefore, it is still the previous SF activity which determines the features of the outflow in our model. An attempt to evaluate the actual mass loss rate of NGC 1705 has been
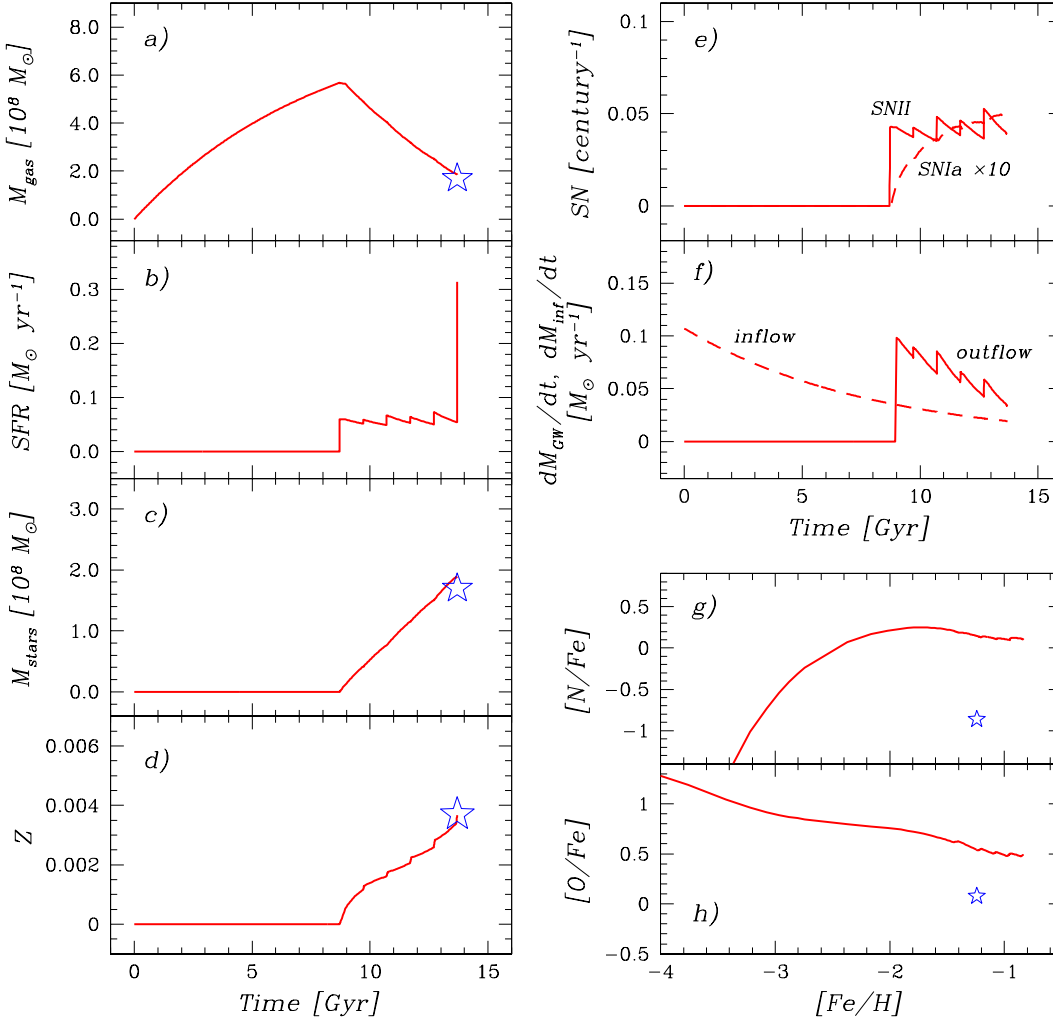
Figure 1. a) $M_{\rm gas}$, b) SFR, c) $M_{\rm stars}$, d) gas metallicity, e) Type II *(solid line)* and Type Ia *(dashed line;* multiplied by a factor of 10 to make it clearly visible) SN rate, f) $\dot{M}_{\rm GW}$ *(solid line)* and $\dot{M}_{\rm inf}$ *(dashed line)* as functions of time; g) [N/Fe] and h) [O,Fe] as functions of [Fe/H] for Model *1aN* for NGC 1705. The stars represent observed values. Both the theoretical and the observed (Aloisi et al. 2005) [el/Fe], [Fe/H] ratios are normalized to solar values by Asplund et al. (2004).

made by Meurer et al. (1992) in their multi-wavelength study of this object. They parameterize the rate of mass loss from the galaxy in terms of two quantities, $M_{\rm flow}$, the total mass of gas entrained in the outflow, and $M_{\rm tot}/L_{\rm B}$, the total mass-to-light ratio. The uncertainty in $M_{\rm flow}$ (nearly three orders of magnitude) and the poorly known DM contribution to $M_{\rm tot}$ make the observed mass loss rate really ill-constrained: Meurer et al. indicate a minimum mass loss rate of 0.0026 $M_\odot$ yr^{-1} [one order of magnitude below our prediction, $\dot{M}_{\rm GW}(t_{\rm now}) \simeq 0.04$ $M_\odot$ yr^{-1}], but values up to three orders of magnitude higher are also permitted. It is thus clear that theoretical models for the development of GWs are poorly constrained by the observations currently available for NGC 1705. In this respect, a much more interesting case to study is NGC 1569, which has its outflow much better characterized by deep *Chandra* spectral imaging (Martin et al. 2002). Therefore, we defer any further consideration on the GW behaviour to Sect. 4.2, where we treat in detail the formation and evolution of NGC 1569.

As mentioned above, we need to assume that the winds driving the evolution of NGC 1705 are differential, i.e., they carry away a large fraction of the newly produced metals, while retaining most of hydrogen. This is necessary in order to reproduce both the observed present-day gas content and the current metallicity of the galaxy. In Model *1aN*, we set the β_i parameters to 2×10^{-5} for the heavy elements and to 2×10^{-6} for the light ones (see Sect. 3.1 and Table 5). Setting β_i to 2×10^{-6} for all the chemical species would result in a present-day metallicity of 0.017, i.e. almost solar. On the contrary, setting β_i to 2×10^{-5} for all the chemical elements would result in a present-day metallicity of 0.04, i.e twice solar, since in this case the metals are mixed in a much lower gaseous mass: $M_{\rm gas}(t_{\rm now}) \sim 3 \times 10^6$ $M_\odot$, at variance with the observations. Clearly, the model is not unique, and the formulation for the $w_i(t)$ parameters is allowed to change. However, in agreement with previous analysis (Pilyugin 1993; Marconi et al. 1994; Recchi et al. 2001, 2004, 2005) we find that models assuming a common value

for $w_i(t)$ (i.e., no differential winds) unavoidably fail to reproduce (at least some of) the observational constraints.

4.1.1 Detailed chemical properties of the neutral and ionized gas phases in NGC 1705

The abundances of oxygen and nitrogen in the local ISM of NGC 1705 have been derived from spectroscopy of H II regions by several groups (see Sect. 2.2.1). In the following, we adopt for comparison with our model predictions the up-to-date values of log(O/H)+12 and log(N/O) suggested by Lee & Skillman (2004 – Fig. 2, *filled diamonds,* with 1- and 2-σ error bars). While the present-day oxygen abundance is very well reproduced by the model (Fig. 2, *upper panel,* cfr. the final points of the tracks), the current N/O ratio is largely overestimated (Fig. 2, *lower panel*). In Fig. 2 we show results obtained by adopting either $x = 1.35$ over the whole stellar mass range *(solid lines)* or $x = 1.6$ above 2 $M_\odot$ *(dashed lines;* Annibali et al. 2003). From now on, we will always refer to models for NGC 1705 as models computed with $x = 1.35$ over the whole stellar mass range.

Recently, *FUSE* and Space Telescope Imaging Spectrograph (STIS) Echelle spectra of NGC 1705 have allowed the determination of the metal (O, Ar, Si, Mg, Al, N, and Fe) abundances also in the neutral medium of NGC 1705 (Aloisi et al. 2005). However, when comparing them to model predictions, one must be aware that saturation (especially for O I), photoionization, contamination by gas laying along the line of sight, depletion into dust grains (e.g., Fe could be more easily locked into grains compared to O) all could affect the derivation of the abundances from the neutral gas (Aloisi et al. 2005). In Fig. 1g,h we display [N/Fe] and [O/Fe] as functions of [Fe/H]. All the ratios are normalized to the solar values of Asplund, Grevesse & Sauval (2004). At [Fe/H] ∼ −1.2, the [N/Fe] predicted by Model *1aN* is higher than the one measured in the neutral gas. This is not unexpected on the basis of the results for the ionized gas phase shown in Fig. 2. The [O/Fe] ratio is overestimated by the model as well. It is worth emphasizing that, while the observed [N/H] and [Fe/H] were corrected for the presence of ionized gas lying along the line of sight, [O/H] was not (Aloisi et al. 2005).

The pronounced discrepancy between model predictions and observations for nitrogen – the predicted nitrogen abundance is sistematically higher than observed, both for the neutral and the ionized gas phases – requires further analysis, especially since the model well reproduces the other reliable observational constraints. In the remaining part of this section, we discuss how current uncertainties in the theories of stellar evolution and nucleosynthesis may affect our results.

4.1.1.1 Less hot bottom burning in intermediate-mass stars?
In Fig. 3 we display the evolution of [N/Fe], [O/Fe] vs. [Fe/H] and log(O/H)+12, log(N/O) vs. time predicted by models for NGC 1705 adopting one of the following combinations: (i) the yields from massive stars by Nomoto et al. (1997) plus the yields from LIMS by van den Hoek & Groenewegen (1997), either with a mass loss parameter along the AGB independent of metallicity – Models *1aN (first column, solid line)* and *1cN (first column, dashed line)* – or with the minimum HBB extent (Model *1aH, second column*); (ii) the yields from massive stars by Woosley & Weaver (1995) plus the yields from LIMS by van den Hoek & Groenewegen (1997) computed with metallicity-dependent mass loss parameter along the AGB (Model *1aW, third column*); (iii) stellar yields by Meynet & Maeder (2002) for rotating stellar models (Models *1aM* and *1cM,*
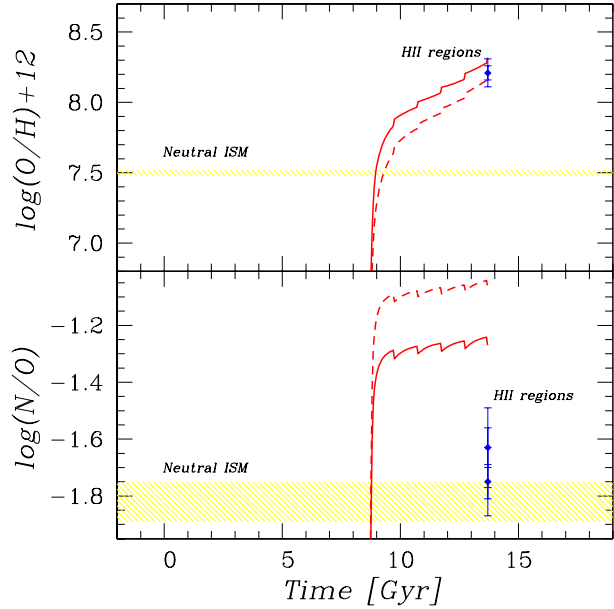

Figure 2. Temporal evolution of oxygen *(top panel)* and nitrogen to oxygen *(bottom panel)* in the ISM of NGC 1705. Predictions from Model *1aN (solid lines:* Salpeter IMF; *dashed lines:* steeper IMF – see text for details) are compared to the available observations. The present-day oxygen abundance of NGC 1705 is that given by Lee & Skillman (2004; mean value of [O III] λ 4363 measurements; *small filled diamond*). The oxygen abundance of the neutral ISM is that derived from far-UV observations (Aloisi et al. 2005; *dashed horizontal band*), not corrected for contamination by ionized gas lying along the line of sight. The current N/O ratio in NGC 1705 is that suggested by Lee & Skillman (2004; *small filled diamonds*), with (lower value) and without (higher value) region B4. A value of log(N/O) = −1.82 ± 0.07 characterizes the neutral phase (Aloisi et al. 2005; *dashed horizontal band*), which is the same as H II regions within the errors.

fourth column, solid and *dashed lines,* respectively). We recall that Meynet & Maeder (2002) have not computed the third dredge-up and HBB phases; hence their stellar models for LIMS are somewhat incomplete. Model *1cN (1cM)* differs from Model *1aN (1aM)* only in the adopted values of the GW efficiencies. Models *1cN* and *1cM* are discussed in detail in Sect. 4.1.2.

Uncertainties in the physics of stellar models for intermediate-mass stars cause the predicted log(N/O) at the present time to vary widely, from −0.9 (Model *1aW*) to −1.5 (Model *1aM*). Stellar models with rotation and without HBB give rise to the lowest theoretical N/O ratios, but they are still only marginally compatible with the observations. Results on the oxygen behaviour are firmer. Yet, lower [O/Fe] ratios are predicted during the whole galaxy evolution when adopting the yields of Woosley & Weaver (1995) rather than those by Nomoto et al. (1997) for massive stars. Meynet & Maeder's yields are the only ones able to reproduce both the observed O/H and N/O at the present time. However, the discrepancies among model predictions and observations for the neutral phase, though sensibly reduced, are not eliminated (Fig. 3, *last column, solid lines*).

4.1.1.2 Localized massive star pollution in NGC 1705?
Notwithstanding the large uncertainties affecting the nitrogen yields, the discrepancy between model predictions about nitrogen evolution in NGC 1705 and the relevant observations is hardly explained only in terms of the adopted stellar yields. A second pos-
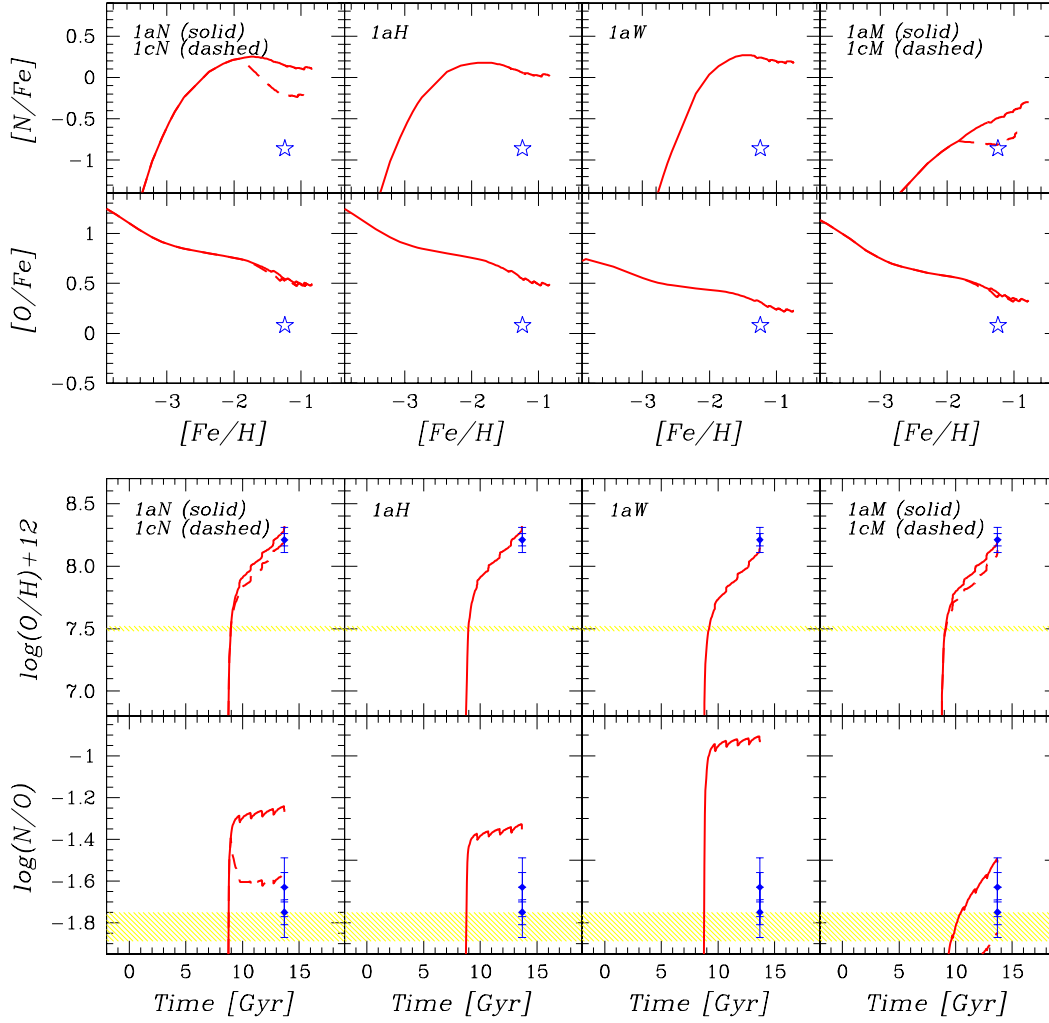
Figure 3. [N/Fe] and [O/Fe] as a function of [Fe/H], log(O/H)+12 and log(N/O) as a function of time. Predictions from Models *1aN, 1aH, 1aW* and *1aM (solid lines)* as well as Models *1cN* and *1cM (dashed lines)* are displayed for comparison one to another and with data for both the neutral (Aloisi et al. 2005; *stars* and *dashed strips*) and ionized gas (Lee & Skillman 2004; *small filled diamonds* with 1- and 2-σ error bars).

sibility is localized self-pollution from dying young massive stars born during the last 3 Myr of SF activity. According to Meynet & Maeder (2002), the N/O ratio in the ejecta of a 60 M$_\odot$ star, having a lifetime of ~ 3.5 million years, is about log(N/O) $\simeq -2.2$ for $Z_{ini} = 0.004$. It would be more interesting to compare to the observations the log(N/O) values predicted for rotating massive stars with lifetimes shorter than 3 million years, but, unfortunately, no star models with initial mass larger than 60 M$_\odot$ are provided yet. Anyway, we notice that the N/O ratio in the ejecta of massive stars with initial metallicity $Z_{ini} = 0.004$ and initial rotational velocity $v_{ini} = 300$ km s^{-1} is a decreasing function of mass (Meynet & Maeder 2002). Therefore, *lower N/O ratios are expected in case of localized massive star self-pollution with respect to the general predictions of homogeneous GCE models,* which may solve the discrepancy between model predictions and observations. However, such a solution would not account for the low nitrogen abundance measured with *FUSE*. Moreover, the constancy of log(O/H)+12 among different H II regions issues a serious challenge to this interpretation.

4.1.2   *The rôle of gas flows*

IMF variations in the range allowed by CMD analyses do not allow to solve the 'nitrogen problem' in NGC 1705 (see Fig. 2, *lower panel*). We are thus left with the possibility that the efficiency of nitrogen ejection through the wind of NGC 1705 is higher than that for oxygen, i.e., $\beta_N/\beta_O \neq 1$. Though this hypothesis needs to be tested by detailed hydrodynamical computations before it can be accepted or rejected, we compute two models for NGC 1705 in which a higher β_N/β_O value is assumed, namely, $\beta_N/\beta_O \simeq 2$ rather than 1 (Models *1cN* and *1cM*), and find that the latter matches fairly well the available observations (Fig. 3, *last column, dashed lines*). In conclusion, it seems that the outflowing gas should be differentially enriched by the products of stellar nucleosynthesis in order to make the model predictions match the observations.

At this point, one must check if our conclusions change by modifying the prescriptions on gas inflows. Up to now, we assumed that some unprocessed gas is continuously accreted by the galaxy
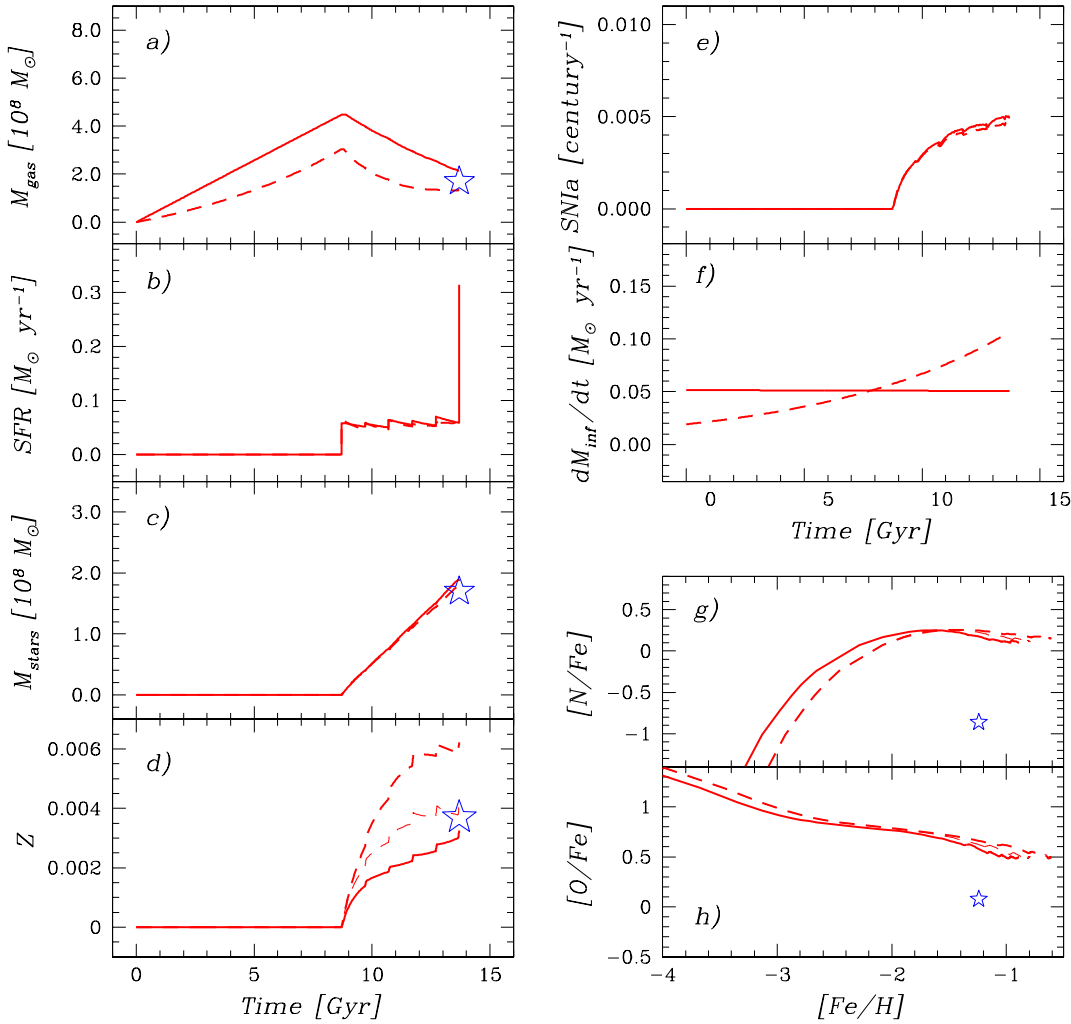
Figure 4. Same as Fig. 1, but for models for NGC 1705 where the infall rate is either constant *(thick solid lines)* or exponentially increasing in time *(thick and thin dashed lines)*. In the latter case, the hypothesis of differential GWs may be relaxed (see text for details).

during the whole Hubble time according to an infall law exponentially decreasing with time[§] and with a time scale $\tau = 8$ Gyr. In the following, we discuss the results obtained when considering an infall rate either constant or exponentially increasing with time (again with $\tau = 8$ Gyr). The latter case would simulate important mergers with gaseous lumps at late times.

Results of models in which either a constant or an increasing infall rate are considered are sketched in Fig. 4. Once a constant infall rate is assumed, predictions from Model *1aN* (Fig. 4, *solid lines*) almost do not differ from those obtained by the same model with a mass accretion rate exponentially decreasing in time (cfr. Fig. 1), except for the current mass loss rate, $\dot{M}_{GW}(t_{now}) = 0.1$ M$_\odot$ yr^{-1}, rather than 0.04 M$_\odot$ yr^{-1}. In the case of constant infall, metals are mixed in a slightly higher gaseous mass $[M_{gas}(t_{now}) = 2.1 \times 10^8$ M$_\odot$ rather than 1.9×10^8 M$_\odot]$, and

---

[§] This is a widely adopted, but completely arbitrary, assumption of GCE models (see, e.g., Mouhcine & Contini 2002 and discussion therein).
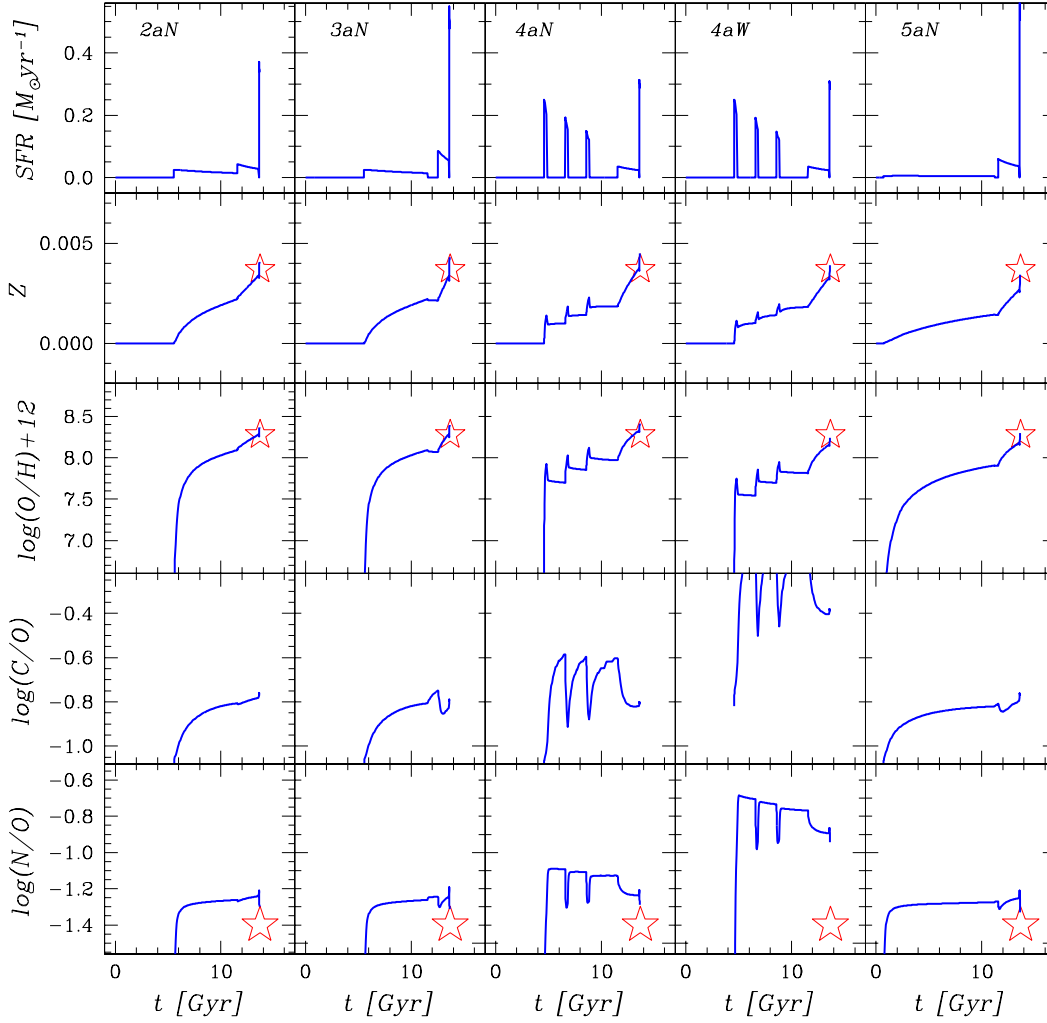
one gets $Z = 0.0032$ rather than $Z = 0.0037$ at the present time, a negligible difference. Instead, if the rate of mass accretion increases in time (see Fig. 4f, *dashed line*), the current gaseous mass of the galaxy is overestimated by the model, unless one does not raise the efficiency of hydrogen loss through the wind. In Fig. 4a we display the behaviour of the gas mass with time predicted by Models *1dN* and *1eN*, both assuming $\beta_i = 0.5 \times 10^{-5}$ for the light elements *(dashed lines)*. This is the highest β_i value for hydrogen ejection we can impose while still retaining enough mass to match the observations. The current metallicity of the ISM is a further constraint to be fulfilled, and it restricts the possible choices of β_i for the heavy elements. As an example, in Fig. 4d we show results obtained with β_i equal to either 2.5×10^{-5} (Model *1dN*, *thin dashed line*) or 1.5×10^{-5} (Model *1eN*, *thick dashed line*) for elements heavier than helium. It is immediately seen that an infall rate exponentially increasing in time allows one to relaxe the differential wind hypothesis: $\beta_{heavy}/\beta_{light} = 10$ for Model *1aN*; $\beta_{heavy}/\beta_{light} = 5$ for Model *1dN* (see also Table 5). At this point,

Figure 5. SFR, global metallicity and CNO abundances as functions of time according to Models *2aN*, *3aN*, *4aN*, *4aW* and *5aN* for NGC 1569. See text for details.

one might wonder whether a fine tuning of model parameters would make the $\beta_{\text{heavy}}/\beta_{\text{light}}$ value further approach unity, eventually getting rid of the need for metal-enriched GWs. We ran several models, but we never reproduced simultaneously both the current gaseous mass and ISM metallicity with $\beta_{\text{heavy}}/\beta_{\text{light}} = 1$, unless making some very *ad hoc* assumptions with possible huge episodes of mass accretion at late times. However, NGC 1705's outer optical isophotes appear round and regular, suggesting a relatively peaceful environment (Meurer et al. 1998). Finally, notice that changing the infall law does not solve the above-mentioned discrepancy between model predictions and observations for nitrogen: models with $\beta_{\text{N}}/\beta_{\text{O}} = 1$ never match the data, independently of the adopted infall rate formulation (cfr. Fig. 4g,h and Fig. 1g,h). The current rate of mass loss predicted by models with rate of gas accretion exponentially increasing with time is $\dot{M}_{\text{GW}}(t_{\text{now}}) = 0.2\ \text{M}_\odot\ \text{yr}^{-1}$, owing to the higher hydrogen mass entrained in the outflow in this case.

4.2 NGC 1569

NGC 1569 is another well-studied, relatively nearby late-type dwarf, whose spectacular GW has been powered by an unusually high-level SF activity (see Sect. 2.2.2). Given the similarities between NGC 1705 and NGC 1569, we find it natural to start a detailed study of NGC 1569 and see whether models adopting the formalism developed for NGC 1705 satisfy the observational constraints available for NGC 1569 as well.

Our models for NGC 1569 all assume that two major bursts of SF have occurred in the last ~ 1–2 Gyr, in agreement with the inferences from the observed CMDs (Greggio et al. 1998; Angeretti et al. 2005). Because of observational uncertainties and since the observed CMDs are relevant to small inner galactic regions – while we need a global SFR referring to the whole galactic area – we still have some degrees of freedom when choosing the actual SFRs at late times. Moreover, we must allow for some SF activity at earlier times, in order to build up a total stellar mass which matches that inferred from the observations. Possible choices are not com-

Table 6. Model results for NGC 1569 (at $t = t_{\rm now} = 13.7$ Gyr; *second* to *twelfth cols.*). The time of the onset of the first GW episode, $t_{\rm GW}$, is also shown *(last col.)*.

Model	$M_{\rm gas}$ (M$_\odot$)	$M_{\rm stars}$ (M$_\odot$)	$M_{\rm tot}$ (M$_\odot$)	$\mu^{\rm a}$	SFR (M$_\odot$ yr^{-1})	Z	(He/H)	log(O/H)+12	log(N/O)	log(C/O)	$\dot{M}_{\rm GW}$ (M$_\odot$ yr^{-1})	$t_{\rm GW}$ (Gyr)
2aN	1.7×10^8	1.4×10^8	3.1×10^8	.55	0.3	0.0041	0.086	8.37	-1.30	-0.77	0.2	6.00
3aN	1.6×10^8	1.4×10^8	3.1×10^8	.53	0.5	0.0043	0.086	8.40	-1.31	-0.80	0.3	6.00
4aN	1.4×10^8	1.3×10^8	2.9×10^8	.53	0.3	0.0045	0.086	8.41	-1.29	-0.81	0.1	4.65
4aW	1.4×10^8	1.3×10^8	3.0×10^8	.53	0.3	0.0039	0.088	8.24	-0.94	-0.39	0.1	4.65
5aN	2.1×10^8	1.2×10^8	3.3×10^8	.63	0.5	0.0034	0.085	8.30	-1.33	-0.77	0.3	2.50
5aH	2.1×10^8	1.2×10^8	3.3×10^8	.63	0.5	0.0034	0.085	8.30	-1.45	-0.74	0.3	2.50
5aM	2.1×10^8	1.2×10^8	3.3×10^8	.63	0.5	0.0029	0.090	8.19	-1.52	-0.63	0.3	2.50

$^{\rm a}$ $\mu = M_{\rm gas}(t_{\rm now})/[M_{\rm gas}(t_{\rm now}) + M_{\rm stars}(t_{\rm now})]$
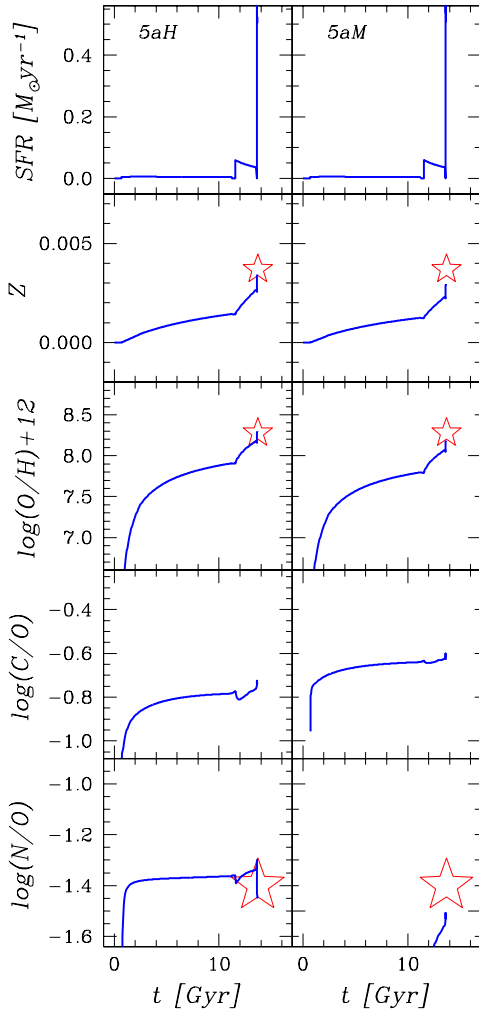
Figure 6. Same as Fig. 5, but for Models *5aH*, *5aM*.

pletely arbitrary, since they must obey two more basic, stringent constraints:

(i) Most of the latest SF activity is concentrated within the area surveyed by Greggio et al. (1998). Therefore, it is safe to adopt the

SFR suggested by those authors, ~ 0.5 M$_\odot$ yr^{-1}, as representative of the overall SF activity across the whole body of the galaxy. Besides this value, we also test the slightly lower one derived by Hunter & Elmegreen (2004) from Hα imaging of NGC 1569, ~ 0.3 M$_\odot$ yr^{-1}.

(ii) SF activity prior to that surveyed by *HST* likely proceeded at much lower rates (see the discussion in Angeretti et al. 2005). Therefore, for ages between ~ 1–2 and ~ 13 Gyr ago, we assume a continuous SF activity, which proceeds at rates much smaller than assumed for the recent episodes. However, only for the sake of comparison with old 'bursting' models, we also examine the case of a bursting SF regime at early times, with three bursts alternating long quiescency periods.

Table 5 summarizes the SFHs assumed in this paper for NGC 1569 in the light of the above considerations (Models from *2* to *5*). Model results are discussed below.

4.2.1 Bursting, gasping or continuous SF regimes?

Figs. 5, 6 and Table 6 summarize and compare the results obtained with different models for NGC 1569 where the SFH and stellar yields are allowed to change one at a time. The adopted structural parameters of the models are: $M_{\rm nor} = 5 \times 10^8$ M$_\odot$, $R_{\rm eff} = 1$ kpc, $M_{\rm d} = 5 \times 10^9$ M$_\odot$, $R_{\rm eff}/R_{\rm d} = 0.1$ (see Sect. 3.1 and Table 4). The infall law is exponentially decreasing with time with $\tau = 0.5$ Gyr for all the models (see, however, Sect. 4.2.3). Models *2aN* and *3aN* assume that a long-lasting SF activity preceded the strong last 1–2 Gyr activity detected with *HST*. Following Greggio et al. (1998) and Angeretti et al. (2005), we assume that the most recent SF activity proceeded through two violent successive bursts: the first started almost 2 (Model *2aN*) to 1 (Model *3aN*) Gyr ago and lasted nearly 2 (Model *2aN*) to 1 (Model *3aN*) Gyr, the second started 100 Myr ago and finished a few Myr ago. A 50 Myr gap separates the two episodes; assuming a longer interburst period (150 Myr – Angeretti et al. 2005) does not change the results. A weaker ($\nu = 0.05$ Gyr^{-1}), but long-lasting ($\Delta t = 6$ Gyr) SF episode is assumed to have occurred from $t = 5.55$ to $t = 11.55$ Gyr, where no detailed information is available from *HST* photometry. This pristine SF raises the metal content of the gas from $Z = 0$ to $Z \simeq 2 \times 10^{-3}$. For Models *4aN* and *4aW*, the most ancient activity consists of three intense short-lasting bursts, while Models *5aN*, *5aH*, *5aM* adopt a continuous, very low-level SFR over almost the whole Hubble time. All the models share the same stellar nucleosynthesis prescriptions, but Models *4aW*, *5aH*, *5aM*. The adopted GW efficiencies are always the same (see Table 5).

First, we want to emphasize that models assuming either a

Table 7. Model results for NGC 1569 (at $t = t_{\text{now}} = 13.7$ Gyr; *fourth* to *twelfth cols.*). Model prescriptions are the same of Model *5aN* (*first row*), except for the adopted SNII and SNIa thermalization efficiencies (*first* and *second cols.*) and, eventually, DM content (*third col.;* see text for more details). The time of the onset of the GW, t_{GW}, is also indicated (*last col.*).

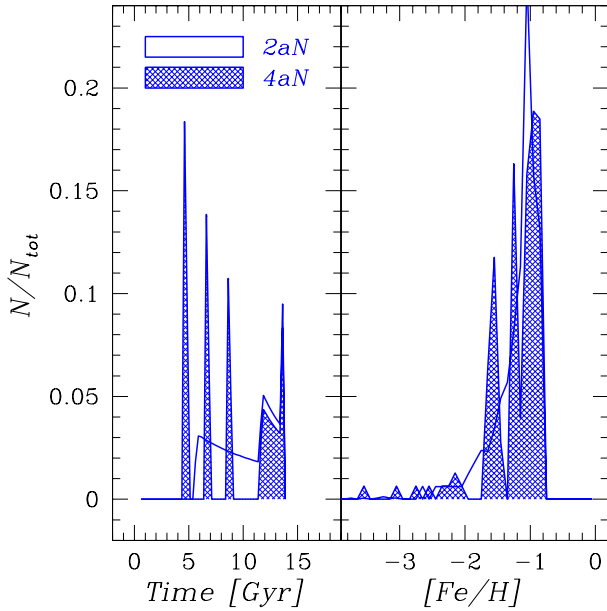| η_{SNII}	η_{SNIa}	$\frac{M_{\text{d}}}{M_{\text{lum}}}$	M_{gas} ($M_{\odot}$)	M_{stars} ($M_{\odot}$)	SFR ($M_{\odot}$ yr^{-1})	Z	(He/H)	log(O/H)+12	log(N/O)	log(C/O)	$\dot{M}_{\text{GW}}$ ($M_{\odot}$ yr^{-1})	t_{GW} (Gyr)
0.20	0.20	10	2.1×10^8	1.2×10^8	0.5	0.0034	0.085	8.30	-1.33	-0.77	0.3	2.50
0.03	1.00	10	2.9×10^8	1.2×10^8	0.5	0.0048	0.085	8.44	-1.29	-0.79	0.09	4.15
0.50	0.50	10	0.8×10^8	1.2×10^8	0.5	0.0035	0.088	8.31	-1.36	-0.71	0.4	1.30
0.50	0.50	50	0.9×10^8	1.2×10^8	0.5	0.0034	0.088	8.29	-1.36	-0.71	0.4	2.00
0.20	0.20	5	2.1×10^8	1.2×10^8	0.5	0.0034	0.085	8.30	-1.33	-0.77	0.3	2.25

Figure 7. Distributions of low-mass, long-lived stars as functions of time (*left panel*) and metallicity (*right panel*) according to Models *2aN* and *4aN* for NGC 1569. The models assume the same SFH in the last ~ 2 Gyr, where more stringent constraints are available from *HST* photometry. As far as earlier activity is concerned, Model *2aN* adopts a continuous, low-level SF over ~ 6 Gyr, while Model *4aN* assumes three short-lasting bursts. On the right-hand panel the two theoretical distributions turn out to be indistinguishable.

bursting, or a gasping, or a fairly continuous, highly variable SF regime are all able to produce results consistent with the observations (e.g., Models *2aN*, *4aN*, *5aN*, Fig. 5, *first, third* and *last col.*, respectively). They provide relatively small differences in the predicted frequency distributions of low-mass stars with metallicity (Fig. 7). Only much deeper CMDs could unveil the 'true' SFH of NGC 1569 at epochs prior to 1–2 Gyr ago. So far, we have some clues that early SF in NGC 1569 went on at rates significantly lower than the ones characterizing later episodes (Angeretti et al. 2005). This information, coupled to current observational evidence pointing to fairly continuous SFHs for most DIGs and BCDs (Schulte-Ladbeck et al. 2001; Annibali et al. 2003; Tosi 2003), leads us to indicate the SFH labelled *5* as the most likely evolutionary scenario for NGC 1569.

Second, we find that for NGC 1569 different combinations of stellar yields reproduce the N/O data (at 2-σ, but fine tuning of model parameters may reconcile model predictions to observations

even better), except for Model *4aW*, adopting the van den Hoek & Gronewegen (1997) yields with metal-dependent η_{AGB} for LIMS. This model indeed largely overestimates the N/O value measured in the local ISM of NGC 1569 [log(N/O) = -1.39 ± 0.05; Kobulnicky & Skillman 1997]. Successful models for NGC 1569 all have $\beta_{\text{N}}/\beta_{\text{O}} = 1$, at variance with models for NGC 1705, where, in order to fit the observations, a value of $\beta_{\text{N}}/\beta_{\text{O}}$ greater than 1 is always required, independently of the choice of the stellar yields.

The issue of the GW efficiencies deserves further considerations. The SF activity in NGC 1569 triggers and sustains an outflow on a galactic scale in our model galaxies. The more efficient is the SF process, the more effective is the wind in removing the newly produced metals, thanks to its dependence on the SN rate. For instance, Model *3aN* (Fig. 5, *second col.*), computed assuming a SF efficiency higher than Model *2aN* (Fig. 5, *first col.*) during the last 1 Gyr, does not overproduce the present-day oxygen content and overall metallicity of the gas even if the β_i values are kept the same, because the efficiency of gas removal is increased in lockstep with the predicted higher Type II plus Type Ia SN rate. In particular, we find that the assumed time modulation of the mass loss rate [Equation (7)] leads to a predicted mass ejection rate at the present time which is of the same order of magnitude of the present-day SFR, in agreement with recent *Chandra* observations (Martin et al. 2002; cfr. *sixth* vs *twelfth col.* in Table 6). This would not be the case if the mass loss rate were simply proportional to the gas content. In that case, the rate of mass loss through the wind would be maximum when the thermal energy equals the binding energy of the gas for the first time, after which it would monotonically decline in time, owing to the lower and lower gas amount left over by the ongoing SF process. In other words, a simple dependence of the outflow rate on the gas mass would not allow to predict enhanced mass loss rates to coincide with enhanced SF episodes, as observed. It is also worth emphasizing that by assuming a GW simply proportional to the SFR (as often found in the literature) one forgets the effect of delayed SNIa explosions and the wind goes to zero as soon as the SF stops.

4.2.2 The energetics of the ISM

The energetics of the ISM is a complicated issue, and no recipes can be found in the literature which treat it without introducing a number of uncertain free parameters. The energy injected into the ISM by a typical massive star through stellar winds during its lifetime is $E_{\text{wind}} \simeq 10^{49}$ erg, to be compared with an initial blast wave energy of $E_{\text{SN}} \simeq 10^{51}$ erg for both SN types. What really matters is the fraction of this energy which is not radiated away and remains effectively stored in the ISM. In previous work on I Zw 18, Recchi et al. (2001, 2004) assigned a low thermalization efficiency of only

3 per cent to SNeII, whereas a much higher value, 100 per cent, was assumed for SNeIa, exploding in a medium already heated by previous SNII activity after a non-negligible time lag from the onset of the SF. However, those values are likely to apply strictly only to the case of single, instantaneous bursts of SF. If the SF is an almost continuous process, $\eta_{\rm SNII}$ must probably be increased (e.g. Strickland & Stevens 2000). Moreover, $\eta_{\rm SNII}$ should vary with time, since it depends on the amount of gas in form of cold clouds at each time (Melioli & de Gouveia Dal Pino 2004). Since we do not follow the exchange of matter between cold and hot gas phases in our models, we cannot state how much gas is in the form of cold clouds at each time. Therefore, we do not vary $\eta_{\rm SNII}$ and $\eta_{\rm SNIa}$ with time, and assume average constant values for these parameters during the whole galaxy evolution. Moreover, we do not treat SF in small (pc-sized) zones, but we assume that the SF process is distributed over the whole physical dimensions of the object, i.e. on kpc scale. Yet, our simplistic models tell us something about the mechanisms regulating dwarf galaxy formation and evolution. In the previous case of NGC 1705, we have assigned the same thermalization efficiency of 20 per cent to stellar winds, SNeII and SNeIa (see Table 4). Here, in the case of NGC 1569, we discuss results from models in which both $\eta_{\rm SNII}$ and $\eta_{\rm SNIa}$ are changed. In two cases, also the prescriptions about the DM content are modified. This affects the depth of the potential well, and thus the time of the onset of the galactic outflow.

In Table 7 we list results from models analogous to Model *5aN* (Table 7, *first row*) as far as the prescriptions about the SFH, stellar nucleosynthesis and GW efficiencies β_i are concerned, but in which different values for $\eta_{\rm SNII}$ and $\eta_{\rm SNIa}$ are adopted. In the extreme case where $\eta_{\rm SNII}$ is set to 0.03 and $\eta_{\rm SNIa}$ is set to 1, the time of occurrence of the GW is delayed ($t_{\rm GW} \simeq 4$ Gyr rather than 2.5 Gyr; Table 7, *last col., first* vs. *second row*). The net outflow rate is reduced, since more weight is given to the less numerous SNeIa, according to Equation (7). As a result, we predict a larger present-day gaseous mass, a higher ISM metallicity at the present time, and a lower mass loss rate, which does not track the SFR any more. This is due to the fact that, while the SNII rate closely follows the SFR, the SNIa rate displays a very different trend. Therefore, while the energy injection from SNeII proceeds in lockstep with the SFR, the bulk of the explosion energy from SNeIa is restored to the ISM with a delay time which depends on the properties of the SF burst. For Model *5aN*, this delay time is ~ 2 Gyr for the early weaker activity and ~ 1 Gyr for the second to last burst. SNIa progenitors born during the most recent SF activity had no time to restore the bulk of their energy into the ISM yet. If one increases the values of the β_i parameters – which are free parameters of the model – in order to reproduce the observational constraints, finds that by assuming higher β_i values ($\sim 5 \times 10^{-6}$ for H, D and He and $\sim 5 \times 10^{-5}$ for the elements heavier than helium) can fit all the available observational constraints, but the present-day mass loss rate, which turns out to be roughly a factor of three lower than the observed present-day SFR. This seems to suggest that $\eta_{\rm SNII} \simeq \eta_{\rm SNIa}$ is a more reasonable choice.

In Table 7 we also show the results obtained in a case where $\eta_{\rm SNII} = \eta_{\rm SNIa} = 0.50$. In this case, a lower present-day gaseous mass survives the SF process (*fourth col., third row*), unless one reduces the strength of the β_i coefficients. It is very difficult to put constraints on the values of the β_i and $\eta_{\rm SNII}$, $\eta_{\rm SNIa}$ parameters separately. In fact, they enter the model in a complex way, i.e. through the products $\beta_i \times \eta_{\rm SNII}$, $\beta_i \times \eta_{\rm SNIa}$, which are then used to weigh the SN rates. The poorly known DM amount and distribution do not seem to cause further complications: in Table 7 we display the

results obtained by a model in which $M_{\rm d}/M_{\rm lum}$ is set to 50 rather than 10 and $\eta_{\rm SNII} = \eta_{\rm SNIa} = 0.50$ (*fourth row*). It can be seen that, although in this case $t_{\rm GW} \simeq 2$ rather than ~ 1 Gyr, the model predictions are almost the same (cfr. *third* vs. *fourth rows* in Table 7), due to the scarce evolution of the system at those early times. Similarly, setting $M_{\rm d}/M_{\rm lum}$ to 5 and $\eta_{\rm SNII} = \eta_{\rm SNIa} = 0.20$ does not affect the model predictions (Table 7, *last row*).

4.2.3 Late accretion of gaseous lumps onto NGC 1569?

It has been suggested (Melioli & de Gouveia Dal Pino 2004) that infall of fresh gas from the surroundings could help to keep the value of the thermalization efficiencies lower than unity. Therefore, we have computed a model (Model *5dN*) in which the infall rate increases with time and the time scale for infall, τ, is set to 5 rather than 0.5 Gyr, simulating a late accretion of gaseous lumps. With this choice, the present-day properties of NGC 1569 are well reproduced (see Fig. 8). The unusually high SFR in NGC 1569 is now explained by the replenishment of the H I reservoir in its disc by newly accreted material. Indeed, some evidence that the galaxy is presently ingesting a small gaseous companion exists (Stil & Israel 1998; Mühle et al. 2005). In particular, according to Mühle et al., the emergence of the latest burst could be explained by the accretion of H I gas with a mass of $\sim 10^7$ M$_\odot$. Our Model *5dN* is characterized by an infall rate $\dot{M}_{\rm inf} \sim 0.1$ M$_\odot$ yr^{-1} during the past 100 Myr, which implies that during this period nearly 10^7 M$_\odot$ of primordial gas are accreted by the galaxy. The predicted outflow rate is $\dot{M}_{\rm GW} \sim 0.6$ M$_\odot$ yr^{-1}, which leads to a total ejected mass of 6.3×10^6 M$_\odot$ over the last 10 Myr, to be compared with an upper limit to the wind mass of 6.2×10^6 M$_\odot$ obtained from spectral fitting (Martin et al. 2002).

4.3 The problem of nitrogen: NGC 1569 vs NGC 1705

Understanding the evolution of nitrogen is one of the major challenges of modern astrophysics. The situation is far from being settled even in our own Galaxy. Recent abundance data for very metal-poor Galactic halo stars (Israelian et al. 2004; Spite et al. 2005) suggest that an important production of primary N took place in the massive halo stars, while the delayed N production from intermediate-mass stars likely overwhelms any massive star contribution at later times (e.g. Chiappini, Romano & Matteucci 2003a). Yet, current massive star models do not produce enough nitrogen to fit the halo data (see Chiappini, Matteucci & Ballero 2005 for an extensive discussion).

Here we find that, while the N/O ratio in the local ISM of NGC 1569 is rather well reproduced by models assuming $\beta_{\rm N}/\beta_{\rm O} = 1$, in order to explain the low N/O ratio measured in H II regions belonging to NGC 1705, it is necessary to assume $\beta_{\rm N}/\beta_{\rm O} \neq 1$. This result is independent of the adopted stellar yields and infall law. Furthermore, when steepening the IMF slope in NGC 1705 as suggested by Annibali et al. (2003; $x = 1.6$ rather than 1.35), the discrepancy between model predictions and observations increases. Before concluding that GWs in NGC 1705 must eject nitrogen more effectively than in NGC 1569, there is one more possibility we have to examine.

4.3.1 IMF variations from galaxy to galaxy?

One may wonder whether coupling an IMF different from Salpeter in NGC 1569 with the same $\beta_{\rm N}/\beta_{\rm O}$ value which matches the N/O
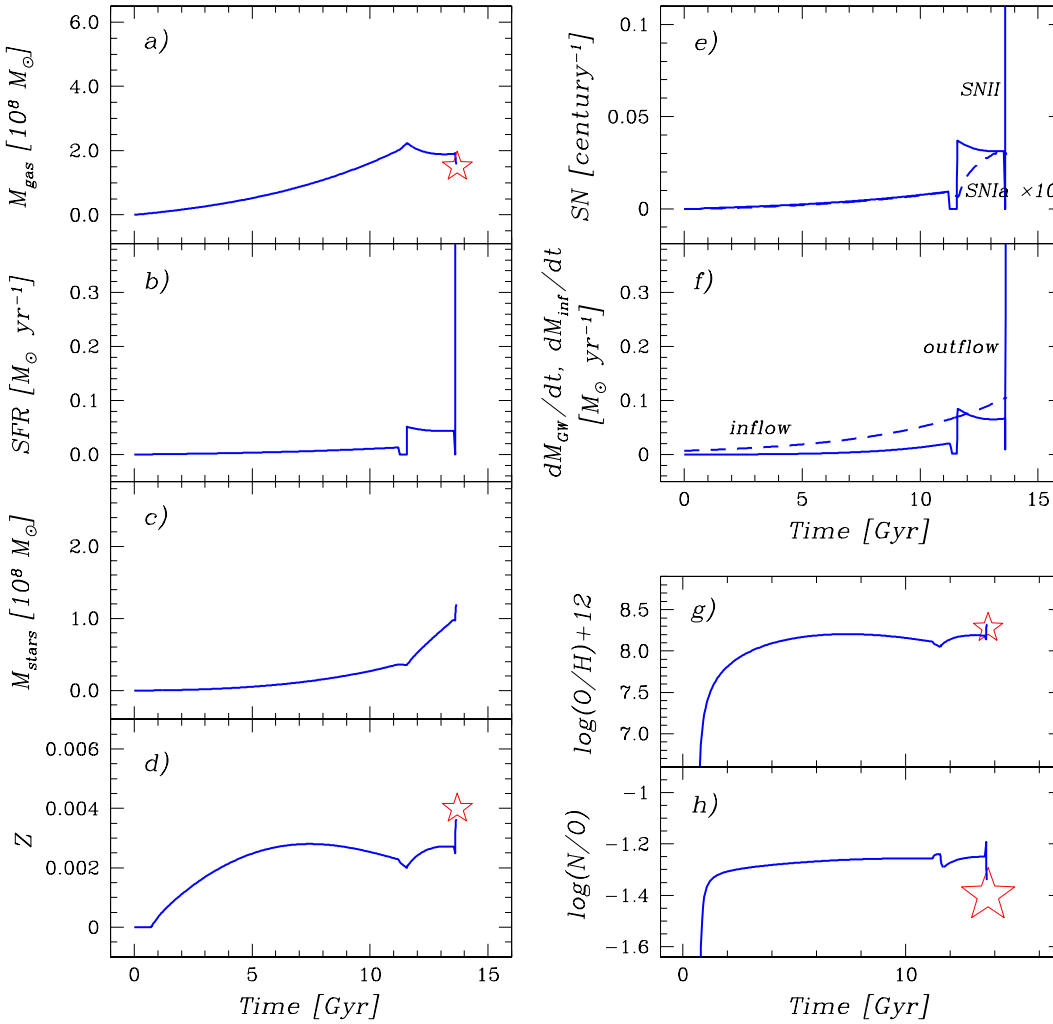
Figure 8. Predictions of Model *5dN* for NGC 1569: a) M_{gas}, b) SFR, c) M_{stars}, d) gas metallicity, e) Type II *(solid line)* and Type Ia *(dashed line;* multiplied by a factor of 10 to make it clearly visible) SN rate, f) $\dot{M}_{\mathrm{GW}}$ *(solid line)* and $\dot{M}_{\mathrm{inf}}$ *(dashed line)* as functions of time; g) log(O/H)+12 and h) log(N/O) as functions of time. The stars represent observed present-time values (see text for details).

data for NGC 1705 would allow to reproduce the N/O ratio measured for NGC 1569 as well. Possible IMF variations in the range of massive and intermediate-mass stars are constrained by *HST* photometry. In particular, for NGC 1569 a power-law exponent flatter than Salpeter's cannot be excluded. Indeed, a value of $x = 0.35$ over the whole stellar mass range still reproduces the red plume of the observed CMD (Angeretti et al. 2005), though it should be cautioned that, due to NICMOS resolution limits, small unresolved stellar clusters might appear as single stars populating the red plume, thus leading to an artificial flattening of the IMF. Besides this, one should always bear in mind that the observed CMDs cannot constrain the IMF below the mass limit given by the galaxy distance and the photometric depth of the images.

In the following, we show results obtained by running modified versions of Model *5aN*, which assume different IMFs, still fullfilling the required photometric properties of NGC 1569. We adopt either $x = 0.35$ over the whole stellar mass range, or a two-slope

IMF consistent with Salpeter down to 0.5 $M_{\odot}$, and then flattening to $x = 0.3$ for $0.1 \leq m/M_{\odot} \leq 0.5$ (Kroupa & Weidner 2005).

The input SFRs are modified accordingly (a straightforward scaling law does not apply – see Angeretti et al. 2005, their figure 6). Extrapolating the SFR below 0.5 $M_{\odot}$ by adopting $x = 0.3$ rather than $x = 1.35$, results in a SFR about 30 per cent lower than assumed up to now (Angeretti et al. 2005). As a consequence, a lower final mass in stars of $M_{\mathrm{stars}}(t_{\mathrm{now}}) \sim 8 \times 10^7$ $M_{\odot}$ and a higher present-day gaseous mass of $M_{\mathrm{gas}}(t_{\mathrm{now}}) \sim 2.5 \times 10^8$ $M_{\odot}$ are predicted by Model *5aN*. The predicted current metallicity of the galaxy is $Z = 0.003$, while the theoretical N/O ratio is almost unchanged, log(N/O) $= -1.33$ at the present time (cfr. Fig. 5, *last col., last row* to Fig. 9, *bottom panel, dashed line*). However, since the SF preceding the last 1–2 Gyr activity unraveled by *HST* is a poorly-constrained parameter of the model, we can enhance it with respect to the prescriptions of Model *5aN*. For example, by setting $\nu = 0.02$ Gyr^{-1} rather than 0.012 Gyr^{-1}, we find a final stellar (gaseous) mass of 1×10^8 $M_{\odot}$ (1.8×10^8 $M_{\odot}$). The final metallic-
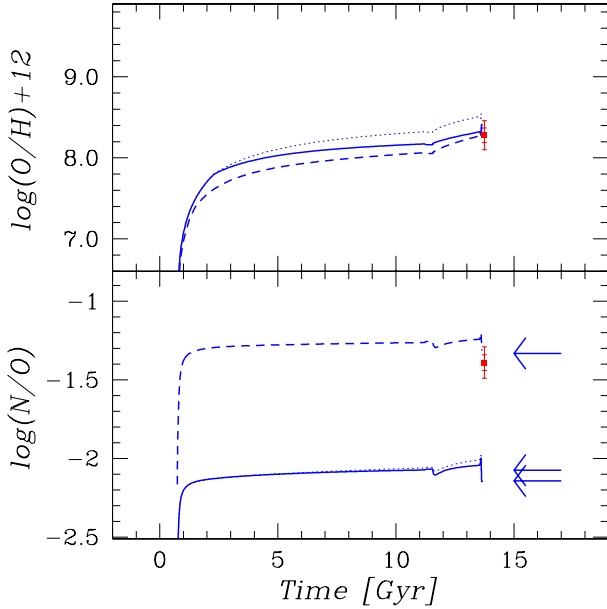
Figure 9. Temporal evolution of oxygen *(top panel)* and nitrogen to oxygen *(bottom panel)* in the ISM of NGC 1569. Model predictions for different IMF slopes [$x = 1.35$ (0.30) above (below) 0.5 $M_\odot$, *dashed lines*; $x = 0.35$ for the whole stellar mass range, *dotted* and *solid lines*) and metal ejection efficiencies ($\beta_i = 2 \times 10^{-5}$, *dashed* and *dotted lines*; $\beta_i \simeq 3 \times 10^{-5}$, *solid lines*) are compared to the available observations (*filled squares; see text*). The ending points of the evolutionary tracks are marked with arrows in the log(N/O) vs. time plot.

ity of the ISM is $Z = 0.004$. Therefore, a two-slope IMF consistent with Salpeter's one above 0.5 $M_\odot$ and flattening below ($x = 0.3$) is permitted by the models.

If we assume instead $x = 0.35$ over the whole stellar mass range, we find a stellar (gaseous) mass of 6×10^6 $M_\odot$ (2.9×10^8 $M_\odot$), whereas a metallicity as high as $Z = 0.006$ is attained, so the model cannot be accepted. Notice that by increasing the metal ejection efficiency (i.e., the β_i parameter value) one can recover the present-day metallicity, but the predicted nitrogen to oxygen abundance ratio is always out of the range allowed by the observations. This can be clearly seen from Fig. 9, where the *dotted lines* stand for a model analogous to Model *5aN*, in which the IMF slope is set to 0.35 rather than 1.35, while the *solid lines* refer to the same model once the metal ejection efficiency is increased in such a way that $Z = 0.004$ at the present time.

In conclusion: (i) IMF variations compatible with the shape of the CMD do not prove useful in solving the puzzle of the different log(N/O) measured for NGC 1569 and NGC 1705; (ii) flattening the IMF for $0.1 < m/M_\odot < 0.5$ in NGC 1569 produces results which still agree with the observations, whereas (iii) adopting a flat IMF over the whole stellar mass range produces results at variance with the observational data. This may be a hint that small unresolved stellar clusters have really been treated as single stars located on the red plume in the CMD analysis. We thus conclude that *different efficiencies of nitrogen ejection through the winds are needed in order to explain both the NGC 1569 and NGC 1705 relevant data.*

5 DISCUSSION AND FUTURE WORK

In this section we extend the previous discussion to the interpretation of the log(N/O) vs. log(O/H)+12 diagram for a wider sample of DIGs and BCDs. In Fig. 10, *upper panel,* we show galaxies for which both oxygen and nitrogen have been measured. The position of NGC 1705 and NGC 1569 in the diagram is given by the big filled diamonds¶ and the big filled square with 2-σ error bars, respectively (see Sect. 2.2 for references). We remind the reader that this is not an evolutionary diagram: it refers to present-time abundances, derived from H II region spectroscopy.

Several features emerge from this diagram. It has been pointed out (Izotov & Thuan 1999) that the N/O ratio is independent of oxygen for BCDs with log(O/H)+12 $\leq$ 7.6. As already discussed by Matteucci & Tosi (1985), this is easily interpreted if the fraction of primary N is at least 30 per cent. Izotov & Thuan interpret this result as an indication for primary nitrogen being produced by the same massive stars which synthesize oxygen. In their view, the small dispersion in N/O at these low metallicities argues against any delayed primary nitrogen production from intermediate-mass stars, thus suggesting that these galaxies are now undergoing their first burst of SF. The delayed release of primary N would not leave its imprints until metallicities 7.6 < log(O/H)+12 < 8.2 are attained, while secondary N production would become important only when galaxies get enriched to log(O/H)+12 $\geq$ 8.2 (see also Henry, Edmunds & Köppen 2000). These mechanisms would be responsible for the scatter in N/O observed at log(O/H)+12 $\geq$ 7.6.

In previous works (Matteucci & Tosi 1985; Marconi et al. 1994; Chiappini et al. 2003a) we were able to populate the observed log(O/H)+12–log(N/O) diagram with model galaxies, without invoking a primary N production from massive stars (see also Henry et al. 2000). We found that dwarf galaxies experiencing an initial burst of SF in the past and a more recent one, or, alternatively, just one SF episode lasting long enough to let intermediate-mass stars have time restoring their nucleosynthesis products, tend to cluster around the N/O 'plateau'. Models in which more than one burst occur populate the high metallicity, high N/O part of the plot (e.g., Chiappini et al. 2003a, their figure 13 and table 5). However, in those models the SFH and IMF were treated as free parameters, a simpler dependence of the outflow rate on the SFR was assumed, and no attempts were made at modelling specific objects.

As far as an important production of primary N from very metal-poor massive stars is concerned, we recall that current massive star models do not predict an amount of primary N sufficient to explain the Galactic halo star data (Chiappini et al. 2005, and references therein). On the other hand, the amount of primary N synthesized in low-metallicity intermediate-mass stars due to the third dredge-up and HBB processes has been probably overestimated (e.g. Chiappini et al. 2003a). Besides the observational data, in Fig. 10 we plot also the predictions from Models *1aM* and *1fH* for NGC 1705, and *5aM* and *5dH* for NGC 1569. In the upper panel, only the ending points of the theoretical tracks are shown *(big crosses)*, whereas in the lower panel the complete evolutive tracks are displayed. NGC 1705 and NGC 1569 show very high SFRs – among the highest ever observed for DIGs and BCDs – and evidence for protracted SFHs in the past. Therefore, it is not surprising that they reach a relatively large metallicity. However,

---

¶ For NGC 1705, both the mean N/O from measurements in all H II regions and that without the extremely low nitrogen abundance of region B4 are considered (see Lee & Skillman 2004).
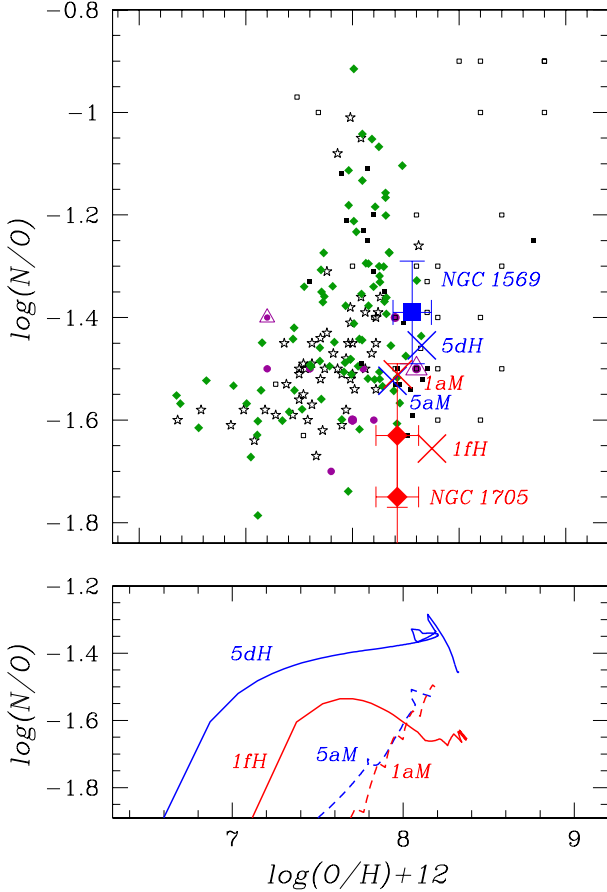
Figure 10. *Upper panel:* log(N/O) vs. log(O/H)+12 diagram for several samples of DIGs, BCDs, and low surface brightness dwarf galaxies. *Filled diamonds:* metal-poor H II galaxies from Kobulnicky & Skillman (1996); *filled circles:* low surface brightness dwarfs from van Zee et al. (1997): bigger circles are objects with higher average SFR in the past; the big empty triangle stands for the sample object with the highest SFR at present – 0.35 $M_\odot$ yr^{-1}, while the small empty one stands for the object with the lowest SFR at present – 0.0015 $M_\odot$ yr^{-1}; *stars:* ground-based spectroscopic observations of 54 supergiant H II regions in 50 low-metallicity BCDs from Izotov & Thuan (1999); *squares:* Virgo DIGs and BCDs from Lee et al. (2003b; *small filled squares*) and Vílchez & Iglesias-Páramo (2003; *small empty squares*). The big diamonds and the big square on the right represent measurements for NGC 1705 and NGC 1569, respectively, along with their 2-σ errors. Also shown are predictions from Models *1aM*, *5aM*, *1fH* and *5dH* (final points of the tracks; *big crosses*). A higher efficiency of nitrogen ejection through the wind is assumed for Model *1fH* with respect to Models *1aM*, *5aM* and *5dH* (see text for details). *Lower panel:* full evolutionary tracks for Models *1aM*, *5aM*, *1fH* and *5dH* in the log(N/O)–log(O/H)+12 space.

NGC 1705 has the lowest N/O ratio observed at those metallicities, and the N/O ratio of NGC 1569 is quite low too, in contrast with previous ideas that DIGs and BCDs evolved through several bursts of SF or experiencing a long-lasting SF regime with a high SF efficiency should populate the high N/O region of the log(O/H)+12–log(N/O) plot. Models *1fH* and *5dH* have been computed with the van den Hoek & Groenewegen (1997) plus Nomoto et al. (1997) yields, for the case of minimum HBB extent. Both assume an infall law exponentially increasing in time. The adopted stellar IMF (Salpeter 1955) and SFHs are consistent with CMD analy-

ses (see previous sections). The case with minimum HBB extent well matches the log(N/O) value actually observed for NGC 1569. However, in order to make the model predictions agree with the observations for NGC 1705 too, one must require that some other mechanism(s) is (are) at work. We argue (Sect. 4.1) that differential galactic outflows in which different fractions of nitrogen are lost with respect to oxygen offer a viable solution. For this reason, Model *1fH* has been computed by assuming $\beta_N/\beta_O \simeq 2$ rather than 1, namely, postulating a higher nitrogen ejection efficiency in the outflow of NGC 1705. Alternatively, in NGC 1705 we might be seeing localized self-pollution from newly-born massive stars. However, the constancy of the oxygen abundance measured in several H II regions of NGC 1705 poses serious challenges to this interpretation (see Sect. 4.1.1.2). Using the yields from rotating star models by Meynet & Maeder (2002) also allows us to fit the data (Fig. 10; Models *1aM* and *5aM*). However, in this case only the highest N/O value for NGC 1705 and the lowest one for NGC 1569 can be explained, rather than *the difference* between the two. When faced with the whole data set, we think that the observed scatter of log(N/O) values at relatively high metallicities needs the hypothesis of differentially enriched GWs in order to be explained. Clearly, only detailed study of a larger number of individual dwarfs, for which the SFH and the IMF had been previously inferred by means of CMD analyses, would allow us to understand the driving processes which lead to the scatter. Recently, our group (PI: A. Aloisi) has been granted time to perform *HST* observations of NGC 4449, a starburst DIG located at a distance $D \simeq$ 4.2 Mpc with log(O/H)+12 = 8.3 and log(N/O) = −1.2 (Sabbadin, Ortolani & Bianchini 1984), i.e., with a N/O ratio higher than both NGC 1569 and NGC 1705. The use of the Advanced Camera for Surveys (ACS) on board *HST* will allow us to reach stars quite fainter than the red giant branch tip (if they exist), and to infer the SFH of NGC 4449 up to several Gyrs ago. We want also to call attention to II Zw 40, a galaxy located at a distance $D \sim 7.5$ Mpc – i.e., within reach of *HST* instrumentation – with log(O/H)+12 = $8.091^{+0.013}_{-0.014}$, log(N/O) = $-1.052^{+0.059}_{-0.077}$, He/H = 0.093 ± 0.013 (Kobulnicky & Skillman 1996), and an old underlying stellar population (Vanzi et al. 1996). Given its very high N/O abundance ratio, it would be an interesting object to study in the context of our research.

6 CONCLUSIONS

In this paper we have presented one-zone chemical evolution models for two dwarf starburst galaxies, NGC 1705 and NGC 1569. For both objects, we have adopted the SFH and IMF previously inferred from *HST* optical and NIR CMDs and found that strong galactic winds develop owing to their violent SF activity. Our main conclusions can be summarized as follows:

(i) The current metallicity of H II regions of both NGC 1705 and NGC 1569 is well reproduced only if strong GWs efficiently remove the metals from the galaxies, in agreement with previous works (e.g., Matteucci & Tosi 1985; Pilyugin 1993; Carigi et al. 1995; Recchi et al. 2001, 2004, 2005).

(ii) The very low N/O ratio measured in NGC 1705 (Lee & Skillman 2004) requires a higher efficiency of nitrogen ejection in the wind of NGC 1705 relative to the wind of NGC 1569 in order to be explained, a result independent of the other parameters of the model. Alternative solutions, such as complete suppression of HBB in intermediate-mass stars or localized chemical pollution

from very massive stars in NGC 1705, are discussed and seem unlikely.

(iii) An offset exists between the oxygen abundance of the neutral phase and that of the ionized gas in NGC 1705, which seems absent in the N/O data (Aloisi et al. 2005). Once some primary nitrogen production through HBB in intermediate-mass stars is allowed for in NGC 1705, an almost constant N/O abundance ratio is predicted in its ISM during almost all the evolution, whereas the oxygen abundance always increases with time (see, e.g., Fig. 3, *first* to *third cols.*). This qualitatively explains why an observational offset should be present in O/H, and absent in N/O, though uncertainties in both the physics of the models and the treatment of the data prevent us from attempting a more quantitative analysis. Notice that by using the yields of Meynet & Maeder (2002), computed by taking into account mass loss and stellar rotation, but neglecting HBB, the theoretical N/O ratio in NGC 1705 steeply increases during its whole evolution (Fig. 3, *last col., last row*). Therefore, in this case the constancy of the N/O ratio in the neutral and ionized gas phases cannot be explained.

(iv) We find hints that *the third dredge-up and HBB must be less effective than assumed up to now in low-metallicity intermediate-mass stars.* We do not find any need for a significant primary nitrogen production from massive stars to explain the present-day abundances in NGC 1705 and NGC 1569. The large primary nitrogen production which characterizes massive stars at $Z_{\rm ini} \leq 10^{-5}$ (see Chiappini et al. 2005) does not leave any imprint on the present-day properties of NGC 1705 and NGC 1569, at $Z \sim 0.004$.

(v) We demonstrate that the efficiency of hydrogen entrainment in the outflow crucially depends on the adopted infall law. If we allow for important mergers with gaseous lumps at late times, we find that the efficiency of hydrogen ejection through the outflow must be of the same order of magnitude as that for the heavy elements in order to fit the observations. On the contrary, with an infall rate exponentially decreasing with time (as usually assumed by GCE models), the required efficiency of hydrogen ejection is up to one order of magnitude lower than that for the heavy elements. While some evidence exists that NGC 1569 could be currently accreting a small companion cloud (Stil & Israel 1998; Mühle et al. 2005), no clear signs of external triggers to the sudden, intense ongoing burst observed in NGC 1705 have been found up to now (Meurer et al. 1998).

(vi) By assuming that the GW efficiency varies in lockstep with the predicted Type II plus Type Ia SN rate, we find $\dot{M}_{\rm GW}(t_{\rm now}) \sim \psi(t_{\rm now})$ in NGC 1569 [where $\dot{M}_{\rm GW}(t_{\rm now})$ and $\psi(t_{\rm now})$ are the current mass loss and SF rates], independently of the assumed infall law and in agreement with observations. The total mass of gas ejected at the average rate predited during the last 10 Myr is 6.3×10^6 M$_\odot$ in the case of an infall rate exponentially increasing with time, while it is 3.5×10^6 M$_\odot$ in the case of an exponentially decreasing infall. These values agree with the best-fitting value (3.5×10^6 M$_\odot$) and upper limit (6.2×10^6 M$_\odot$) for the mass ejected in the outflow given by Martin et al. (2002). Current estimates of the gas mass in the outflow of NGC 1705 vary by almost three orders of magnitude, going from $\dot{M}_{\rm GW}(t_{\rm now}) \simeq 0.0026$ M$_\odot$ yr^{-1} up to ~ 5 M$_\odot$ yr^{-1} (Meurer et al. 1992). These values do not usefully constrain our models, which predict mass loss rates ranging from $\dot{M}_{\rm GW}(t_{\rm now}) \simeq 0.04$ to 0.2 M$_\odot$ yr^{-1}, depending on the adopted infall law prescriptions.

Clearly, we need to apply our models to a larger galaxy sample before drawing firmer conclusions about late-type dwarf galaxy formation and evolution. We identify NGC 4449 and II Zw 40 as promising candidates: owing to their metallicities, similar to those of NGC 1705 and NGC 1569, but higher N/O ratios, they probe a different locus in the log(N/O) vs. log(O/H)+12 plane. Thus, they could help us to unravel the origin of the observed spread among N/O values at a given metallicity. In particular, our group has already been granted *HST* time to perform ACS observations of NGC 4449. These will enable us to determine its SFH and IMF, a necessary step to work out the appropriate chemical evolution models.

REFERENCES

Aloisi A., Clampin M., Diolaiti E., Greggio L., Leitherer C., Nota A., Origlia L., Parmeggiani G., Tosi M., 2001, AJ, 121, 1425

Aloisi A., Heckman T. M., Hoopes C. G., Leitherer C., Savaglio S., Sembach K. R., 2005, in de Grijs R., González Delgado R. M., eds, Starbursts: From 30 Doradus to Lyman Break Galaxies. Springer, Dordrecht, p. P2

Aloisi A., Tosi M., Greggio L., 1999, AJ, 118, 302

Anders P., de Grijs R., Fritze-v. Alvensleben U., Bissantz N., 2004, MNRAS, 347, 17

Angeretti L., Tosi M., Greggio L., Sabbi E., Aloisi A., Leitherer C., 2005, AJ, in press (astro-ph/0504281)

Annibali F., Greggio L., Tosi M., Aloisi A., Leitherer C., 2003, AJ, 126, 2752

Aparicio A., Gallart C., 2004, AJ, 128, 1465

Asplund M., Grevesse N., Sauval A. J., 2004, in Bash F. N., Barnes T. G., eds, ASP Conf. Ser., Cosmic Abundances as Records of Stellar Evolution and Nucleosynthesis. Astron. Soc. Pac., San Francisco, in press (astro-ph/0410214)

Bradamante F., Matteucci F., D'Ercole A., 1998, A&A, 337, 338

Campos-Aguilar A., Moles M., 1991, A&A, 241, 358

Cannon J. M., McClure-Griffiths N. M., Skillman E. D., Côté S., 2004, ApJ, 607, 274

Carigi L., Colín P., Peimbert M., 1999, ApJ, 514, 787

Carigi L., Colín P., Peimbert M., Sarmiento A., 1995, ApJ, 445, 98

Chiappini C., Matteucci F., Ballero S.K., 2005, A&A, 437, 429

Chiappini C., Matteucci F., Gratton R., 1997, ApJ, 477, 765

Chiappini C., Matteucci F., Meynet G., 2003b, A&A, 410, 257

Chiappini C., Romano D., Matteucci F., 2003a, MNRAS, 339, 63

de Marchi G., Clampin M., Greggio L., Leitherer C., Nota A., Tosi M., 1997, ApJ, 479, L27

D'Ercole A., Brighenti F., 1999, MNRAS, 309, 941

De Young D. S., Gallagher J. S. III, 1990, ApJ, 356, L15

Gallart C., Aparicio A., Chiosi C., Bertelli G., Vílchez J. M., 1994, ApJ, 425, L9

Galliano F., Madden S. C., Jones A. P., Wilson C. D., Bernard J.-P., Le Peintre F., 2003, A&A, 407, 159

Gerola H., Seiden P. E., Schulman L. S., 1980, ApJ, 242, 517

González Delgado R. M., Leitherer C., Heckman T. M., Cerviño M., 1997, ApJ, 483, 705

Greggio L., Tosi M., Clampin M., de Marchi G., Leitherer C., Nota A., Sirianni M., 1998, ApJ, 504, 725

Heckman T. M., Dahlem M., Lehnert M. D., Fabbiano G., Gilmore D., Waller W. H., 1995, ApJ, 448, 98

Heckman T. M., Leitherer C., 1997, AJ, 114, 69

Heckman T. M., Sembach K. R., Meurer G. R., Strickland D. K., Martin C. L., Calzetti D., Leitherer C., 2001, ApJ, 554, 1021

Henry R. B. C., Edmunds M. G., Köppen J., 2000, ApJ, 541, 660

Hensler G., Köppen J., Pflamm J., Rieschick A., 2004, in Duc P.-A., Braine J., Brinks E., eds, Proceedings of the 217th IAU Symposium. Astron. Soc. Pac., San Francisco, p. 178

Hill V., 2004, in McWilliam A., Rauch M., eds, Origin and Evolution of the Elements. Cambridge Univ. Press, Cambridge, p. 205

Hodge P. W., 1971, ARA&A, 9, 35

Hoffman G. L., Brosch N., Salpeter E. E., Carle N. J., 2003, AJ, 126, 2774

Hunter D. A., Gallagher J. S. III, 1985, ApJS, 58, 533

Hunter D. A., Elmegreen B. G., 2004, AJ, 128, 2170

Israel F. P., 1988, A&A, 194, 24

Israelian G., Ecuvillon A., Rebolo R., García-López R., Bonifacio P., Molaro P., 2004, A&A, 421, 649

Izotov Y. I., Thuan T. X., 1998, ApJ, 500, 188

Izotov Y. I., Thuan T. X., 1999, ApJ, 511, 639

Izotov Y. I., Thuan T. X., 2004, ApJ, 616, 768

Kobulnicky H. A., Skillman E. D., 1996, ApJ, 471, 211

Kobulnicky H. A., Skillman E. D., 1997, ApJ, 489, 636

Kobulnicky H. A., Skillman E. D., 1998, ApJ, 497, 601

Köppen J., Edmunds M. G., 1999, MNRAS, 306, 317

Kroupa P., Weidner C., 2005, in R. Cesaroni et al., eds, Proceedings of the 227th IAU Symposium, Massive Star Birth, in press (astro-ph/0507582)

Kunth D., Sargent W. L. W., 1986, ApJ, 300, 496

Larson R. B., Tinsley B. M., 1978, ApJ, 219, 46

Lee H., McCall M. L., Kingsburgh R. L., Ross R., Stevenson C. C., 2003a, AJ, 125, 146

Lee H., McCall M. L., Richer M. G., 2003b, AJ, 125, 2975

Lee H., Skillman E. D., 2004, ApJ, 614, 698

Legrand F., Kunth D., Roy J.-R., Mas-Hesse J. M., Walsh J. R., 2000, A&A, 355, 891

Mac Low M.-M., Ferrara A., 1999, ApJ, 513, 142

Makarova N. L., Karachentsev I. D., 2003, Astrophysics, 46, 144

Marcolini A., Brighenti F., D'Ercole A., 2004, MNRAS, 352, 363

Marconi G., Matteucci F., Tosi M., 1994, MNRAS, 270, 35

Marlowe A. T., Heckman T. M., Wyse R. F. G., Schommer R., 1995, ApJ, 438, 563

Martin C. L., 1996, ApJ, 465, 680

Martin C. L., 1997, ApJ, 491, 561

Martin C. L., Kobulnicky H. A., Heckman T. M., 2002, ApJ, 574, 663

Matteucci F., Chiosi C., 1983, A&A, 123, 121

Matteucci F., Greggio L., 1986, A&A, 154, 279

Matteucci F., Tosi M., 1985, MNRAS, 217, 391

Melioli C., de Gouveia Dal Pino E. M., 2004, A&A, 424, 817

Méndez D. I., Esteban C., 2000, A&A, 359, 493

Meurer G. R., Freeman K. C., Dopita M. A., Cacciari C., 1992, AJ, 103, 60

Meurer G. R., Staveley-Smith L., Killeen N. E. B., 1998, MNRAS, 300, 705

Meynet G., Maeder A., 2002, A&A, 390, 561

Mouhcine M., Contini T., 2002, A&A, 389, 106

Mühle S., Klein U., Wilcots E. M., Hüttemeister S., 2005, AJ, in press (astro-ph/0504229)

Murakami I., Babul A., 1999, MNRAS, 309, 161

Noeske K. G., Iglesias-Páramo J., Vílchez J. M., Papaderos P., Fricke K. J., 2001, A&A, 371, 806

Nomoto K., Hashimoto M., Tsujimoto T., Thielemann F.-K., Kishimoto N., Kubo Y., Nakasato N., 1997, Nucl. Phys. A, 616, 79c

O'Connell R. W., Gallagher J. S. III, Hunter D. A., 1994, ApJ, 433, 65

Olive K. A., Skillman E. D., 2004, ApJ, 617, 29

Origlia L., Leitherer C., Aloisi A., Greggio L., Tosi M., 2001, AJ, 122, 815

Östlin G., 2000, ApJ, 535, L99

Pagel B. E. J., 1997, Nucleosynthesis and chemical evolution of galaxies. Cambridge Univ. Press, Cambridge

Pagel B. E. J., Terlevich R. J., Melnick J., 1986, PASP, 98, 1005

Pantelaki I., Clayton D. D., 1987, in Thuan T. X., Montmerle T., Tran Thanh Van J., eds, Starburts and galaxy evolution. Editions Frontières, Gif-sur-Yvette, p. 145

Peimbert M., Torres-Peimbert S., 1974, ApJ, 193, 327

Pilyugin L. S., 1993, A&A, 277, 42

Pustilnik S. A., Kniazev A. Y., Lipovetsky V. A., Ugryumov A. V., 2001, A&A, 373, 24

Recchi S., Matteucci F., D'Ercole A., 2001, MNRAS, 322, 800

Recchi S., Matteucci F., D'Ercole A., Tosi M., 2004, A&A, 426, 37

Recchi S., Hensler G., Angeretti L., Matteucci F., 2005, A&A, submitted

Romano D., Tosi M., Matteucci F., Chiappini C., 2003, MNRAS, 346, 295

Sabbadin F., Ortolani S., Bianchini A., 1984, A&A, 131, 1

Salpeter E. E., 1955, ApJ, 121, 161

Sancisi R. 1999, in Barnes J. E., Sanders D. B., eds, Proceedings of the 186th IAU Symposium, Galaxy Interactions at Low and High Redshift, p. 71

Sandage A., Hoffman G. L., 1991, ApJ, 379, L45

Scalo J. M., 1986, Fund. Cosmic Phys., 11, 1

Schulte-Ladbeck R. E., Hopp U., Greggio L., Crone M. M., Drozdovsky I. O., 2001, Ap&SSS, 277, 309

Searle L., Sargent W. L. W., Bagnuolo W. G., 1973, ApJ, 179, 427

Sirianni M., Meurer G., Homeier N., Clampin M., Kimble R., The ACS Science Team, 2005, in de Grijs R., González Delgado R. M., eds, Starbursts: From 30 Doradus to Lyman Break Galaxies. Springer, Dordrecht, p. P41

Spite M., Cayrel R., Plez B., et al., 2005, A&A, 430, 655

Stil J. M., Israel F. P., 1998, A&A, 337, 64

Stil J. M., Israel F. P., 2002, A&A, 392, 473

Storchi-Bergmann T., Calzetti D., Kinney A. L., 1994, ApJ, 429, 572

Strickland D. K., Stevens I. R., 2000, MNRAS, 314, 511

Thielemann F.-K., Nomoto K., Hashimoto M., 1993, in Prantzos N., et al., eds, Origin and Evolution of the Elements. Cambridge Univ. Press, Cambridge, p. 297

Tolstoy E., Irwin M., Cole A., Fraternali F., Szeifert T., Marconi G., 2004, The Messenger, 115, 32

Tolstoy E., Saha A., 1996, ApJ 462, 672

Tosi M., 2003, Mem. Soc. Astron. It. Suppl., 3, 137

Tosi M., Greggio L., Marconi G., Focardi P., 1991, AJ, 102, 951

Tosi M., Sabbi E., Bellazzini M., Aloisi A., Greggio L., Leitherer C., Montegriffo P., 2001, AJ, 122, 1271

Vallenari A., Bomans D. J., 1996, A&A, 313, 713

van den Bergh S., 1977, in Tinsley B. M., Larson R. B., eds, Evolution of Galaxies and Stellar Populations. Yale Univ. Obs., New Haven, p. 19

van den Hoek L. B., Groenewegen M. A. T., 1997, A&AS, 123, 305

van Zee L., Haynes M. P., Salzer J. J., 1997, AJ, 114, 2497

van Zee L., Skillman E. D., Salzer J. J., 1998, AJ, 116, 1186

Vanzi L., Rieke G. H., Martin C. L., Shields J. C., 1996, ApJ, 466, 150

Veilleux S., Shopbell P. L., Rupke D. S., Bland-Hawthorn J., Cecil G., 2003, AJ, 126, 2185

Vílchez J. M., Iglesias-Páramo J., 2003, ApJS, 145, 225

Waller W. H., 1991, ApJ, 370, 144

Woosley S. E., Weaver T. A., 1995, ApJS, 101, 181